Review



# Coated and Hybrid Silicon Carbide Nanowires: Advanced Surface Engineering, Interface Control and Functional Applications

Minahil Ishtiaq , Bin Li * , Xiaoyu Shen , Yuanhui Liu , Huan Lin , Bo Zhang , Junhong Chen *

Posted Date: 9 May 2026

doi: 10.20944/preprints202605.0609.v1

Keywords: SiC nanowires; interface engineering; surface coating; heterojunctions

 doi:10.20944/preprints202605.0609.v1



*Review*

# Coated and Hybrid Silicon Carbide Nanowires: Advanced Surface Engineering, Interface Control and Functional Applications

**Minahil Ishtiaq [1], Bin Li [1,*], Xiaoyu Shen [1], Yuanhui Liu [1], Huan Lin [1], Bo Zhang [2] and Junhong Chen [1,*]**

[1] School of Materials Science and Engineering, University of Science and Technology Beijing, Beijing 10083, China
[2] Shandong Jiulong New Materials Co., Ltd., Jinan 256510, China
* Correspondence: libin@ustb.edu.cn (B.L.); cjh2666@126.com (J.C.)

**Abstract**

Silicon carbide (SiC) nanowires possess unique one-dimensional structural features, excellent mechanical strength, thermal stability and wide bandgap properties, showing great potential in high-temperature electronics, catalysis, sensing and composite reinforcement. Nevertheless, pristine SiC nanowires suffer from inert surface activity, weak interfacial compatibility and limited optoelectronic and catalytic performance. Surface coating and heterojunction engineering are effective strategies to address these deficiencies. This review systematically summarizes the synthesis routes of pristine SiC nanowires, including carbothermal reduction, chemical vapor deposition, template-assisted growth and molten salt synthesis, as well as their morphological regulation, physicochemical properties and inherent limitations. Meanwhile, typical coating methods such as wet chemical, hydrothermal, CVD and PIP are elaborated, and the influences of coating thickness, uniformity, adhesion and lattice/thermal compatibility on performance are summarized. The classification and interfacial charge mechanism of Type II, Z-scheme and Schottky heterojunctions are discussed, and the advances of coated SiC nanowires in photodetection, photocatalysis, gas sensing, electromagnetic shielding and energy storage are reviewed. Current challenges including coating stability, scalable preparation and integration bottlenecks are pointed out, and future research directions focusing on interface control, multifunctional integration and AI-assisted material design are prospected.

**Keywords:** SiC nanowires; interface engineering; surface coating; heterojunctions

## 1. Introduction

The nanowires and other nanostructures based on one-dimensional (1D) have garnered much attention due to their directional electron transport, high surface-to-volume ratio, and tunable mechanical and optoelectronic properties [1]. These characteristics made them ideal to be used in energy conversion, composite reinforcement, sensing and nanoelectronics [2–4]. SiC nanowires are extremely resistant to mechanical, thermal, chemical strains and have a bandgap of approximately 2.4–3.2 eV. This renders them suitable to employ in high power electronic systems, nuclear power plants, and aerospace [5,6].

They are produced through controlled chemical routes and have been widely investigated as reinforcing components. Their high aspect ratio, combined with their reported high stiffness and strength [7], makes them attractive for mechanical strengthening across a wide range of matrix systems [8]. Their thermal and structural stability further supports their use in composite systems operating under corrosive and high-temperature conditions [9,10]. Beyond structural reinforcement, SiC nanowires are also under increasing investigation for functional applications including

 doi:10.20944/preprints202605.0609.v1



photocatalysis, energy conversion and storage, gas sensing, and electromagnetic interference shielding [11,12].

SiC nanowires possess multiple performance restrictions even if they exhibit certain useful characteristics. Among these are low surface reactivity, weak interaction with some matrix materials, and insufficient catalytic or optoelectronic efficiency in isolated form. These flaws could affect their performance in uses where interfacial interactions as well surface activity are essential [13,14]. Researchers have sought surface modification methods including oxide or semiconductor coatings to solve these problems to increase chemical interaction, enhance charge transfer, and extend their use range.

Recent research utilized different material coatings and introduced hybrid systems to improve charge transport, chemical interaction, and environmental durability of SiC nanowires. For high-temperature structural composites , oxide-coated SiC nanowires have shown improved oxidation resistance and thermal stability [15], while g-$C_3N_4$-coated SiC nanowires have demonstrated visible-light-driven photocatalytic hydrogen evolution with enhanced charge separation efficiency [16]. Furthermore, improved photocurrent generation and environmental sensitivity in optoelectronic platforms was made possible by SiC-based heterostructures [17]. Advances in interfacial bonding, charge mobility, and band alignment lead to these enhancements. Precision control over coating thickness, shape, and crystallinity made possible by deposition techniques including atomic layer deposition (ALD), chemical vapour deposition (CVD), and hydrothermal synthesis allows to enable application-specific integration [18].

This review provides a comprehensive overview of recent progress in the synthesis and surface modification of SiC nanowires. The main fabrication routes, coating strategies, and surface-engineering approaches are systematically discussed. Particular attention is given to heterojunction design, interfacial behavior, and their influence on application-specific performance. The review also critically addresses the key challenges of scalability, coating stability, and long-term device reliability in applications such as photocatalysis, electronics, sensing, and structural composites.

## 2. Fundamental Aspects of Pristine SiC Nanowires: Synthesis, Structure, and Properties

The pristine SiC nanowires have a high aspect ratio, structural integrity, and extreme condition resistance which is noteworthy. They stay tailored to the advanced applications because of their unique combination of mechanical, electrical and thermal properties. This section covers the key synthesis methods, structural properties and primary properties of uncoated SiC nanowires to understand the functionality of the property prior to surface modification.

### *2.1. Synthesis Techniques*

Synthesis of SiC nanowires has been pursued using different vapor-phase and solution-based approaches each having different benefits with regard to scaling, morphology, crystallinity and purity. The synthesis strategy is frequently dictated by the property and the desired application of the resulting nanowires.

#### 2.1.1. Carbothermal Reduction

Carbothermal reduction is one of the most widely used routes for the synthesis of SiC nanowires. The process involves high-temperature reactions between silica ($SiO_2$) and carbon, typically at 1400 ~1600 °C, and proceeds via the formation of gaseous SiO and CO intermediates. Among the reactions involved, equation. (1) mainly accounts for the generation of these gaseous species, whereas equation (2) and (3), are regarded as the dominant pathway for SiC formation [19].

$$SiO_2(s) + C(s) \rightarrow SiO(g) + CO(g) \quad (1)$$

$$\Delta_r G^{\theta} = (-0.3352T + 678.5016)\ kJ \cdot mol^{-1}$$

 doi:10.20944/preprints202605.0609.v1



$$SiO(g) + 2C(s) \rightarrow SiC(s) + CO(g) \quad (2)$$

$$\Delta_r G^{\theta} = (0.0013T - 79.4950)\ kJ \cdot mol^{-1}$$

$$SiO(g) + 3CO(s) \rightarrow SiC(s) + 2CO_2(g) \quad (3)$$

$$\Delta_r G^{\theta} = (0.3442T - 412.1637)\ kJ \cdot mol^{-1}$$

To clarify the growth mechanism, Liu et al. combined experimental investigation with first-principles molecular dynamics to examine the formation of SiC nanowires at 1550 °C using a $SiO_2$/carbon black molar ratio of 1:6. They reported a higher nanowire yield in BN crucibles than in graphite crucibles, which was attributed to the stronger interaction of BN with the SiO and CO intermediates. These gaseous species were found to condense in the downstream region and promote non-catalytic vapor-phase growth, leading to the formation of both linear and chain-beaded SiC nanowires [19]. Building on this growth framework, Shen et al. further refined the carbothermal route by employing a two-step thermal schedule, in which the system was first heated to 1600 °C to induce SiC nucleation and then maintained at 1350 °C to sustain nanowire growth. This strategy yielded ultrathin 3C-SiC core-shell nanowires with reduced stacking faults and enhanced photoluminescence, highlighting the important role of thermal scheduling in controlling growth kinetics, defect density, and structural quality. The corresponding two-stage growth mechanism is schematically illustrated in Figure 1 [20].

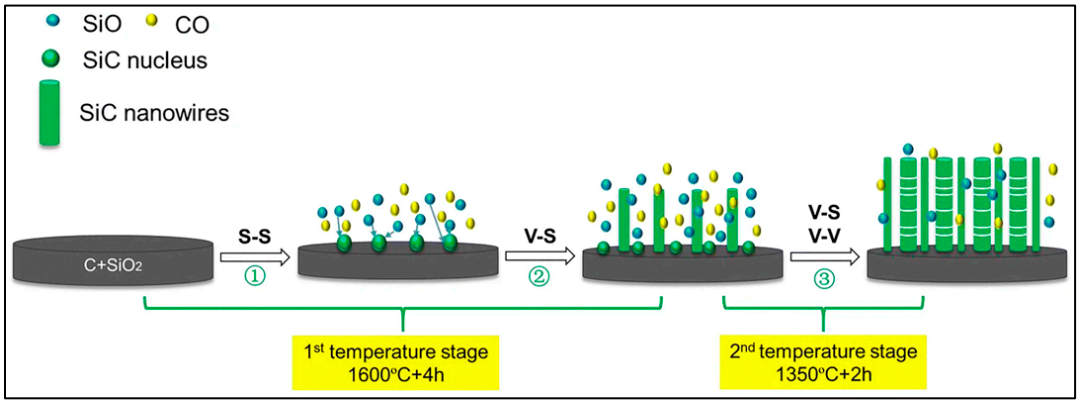


**Figure 1.** Schematic representation of the two-stage carbothermal growth mechanism of SiC nanowires, highlighting nucleation during the first stage at 1600 °C and sustained nanowire growth during the second stage at 1350 °C. Reproduced with permission from Shen et al. [20]. © Springer Nature.

Carbothermal reduction can also evolve from a non-catalytic process into a hybrid growth mode when metallic species are intentionally introduced. Yang et al. reported a combined solid–liquid–solid (SLS) and vapor–liquid–solid (VLS) mechanism in a Fe–Si alloy system, in which Si and Fe formed a liquid alloy layer on graphite at 1600 °C. Carbon from the substrate dissolved into this melt to initiate SiC formation, while vapor-phase SiO and CO were subsequently incorporated into the alloy droplets to sustain nanowire elongation through a VLS process [21]. Lee et al. reported that a mixture of low-purity $SiO_2$ and carbon produced SiC nanowires at 1400 °C through carbothermal reduction. In this system, the Fe-containing impurity present in the silica acted as the catalyst, promoting localized nanowire growth through a transient VLS process, even though no external catalyst was intentionally introduced [22]. This observation demonstrated how the process is sensitive to changes in composition of the precursor. In a similar study by Yao et al., the growth of β-SiC nanowires within the SiC ceramics was achieved through the Fe–Ni-facilitated VLS growth at 1000 and 1100 °C, whereas increasing the temperature (1300 and above) led to vapor-solid growth through catalyst evaporations [23].

All these results indicate that the carbothermal reduction, despite being essentially a vapor-phase method, is highly tunable. It can be used to control nanowire morphology and structure by

 doi:10.20944/preprints202605.0609.v1



modifying thermal conditions and precursor chemistry, and can be used in non-catalytic gas-solid reactions, or with a transient catalytic effect, to achieve control of nanowire morphology and structure.

2.1.2. Chemical Vapor Deposition (CVD)

CVD is a widely used technique that relies on the thermal decomposition or chemical reaction of gaseous precursors on a heated substrate to deposit solid materials. It enables large-scale production of high-purity SiC nanowires with good control over morphology.

Liu et al. synthesized β-SiC nanowires with an amorphous $SiO_2$ sheath using a simplified catalyst-free CVD method at 1300 °C [24]. A mixture of Si and $SiO_2$ powders was milled, placed in a graphite crucible, and enclosed within a corundum crucible filled with graphite powder. Upon heating, Si reacted with $SiO_2$ to generate SiO vapor in situ, and the resulting SiO then reacted with carbonaceous species, including carbon and CO, to form SiC nanowires through a vapor–solid growth process. The obtained product consisted of a crystalline SiC core coated with an amorphous $SiO_2$ sheath, as illustrated in Figure 2.

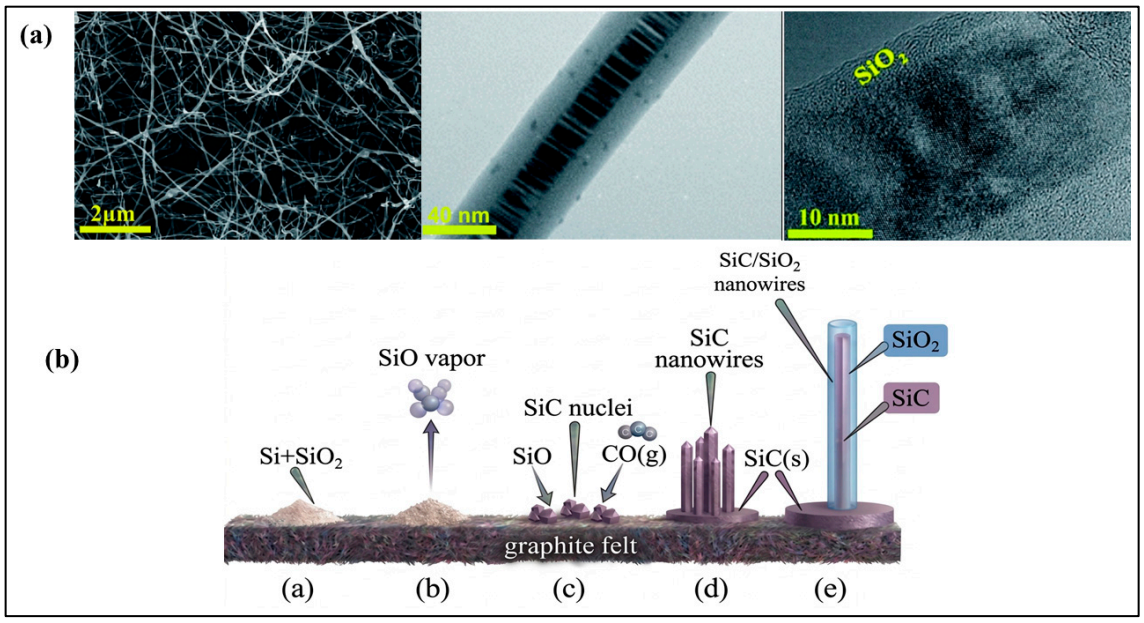


**Figure 2.** (a) SEM and TEM images and (b) proposed growth mechanism of $SiC/SiO_2$ nanowires. (a) Reproduced and (b) adapted with permission from Liu et al. [24] © Royal Society of Chemistry.

Similarly, β-SiC nanowires were synthesized on C/C substrates using methyltrichlorosilane and hydrogen at 1050–1150 °C, where Fu et al. demonstrated a vapor-solid growth mechanism without the use of metal catalysts; oxidation led to the formation of a surface $SiO_2$ layer [25]. In another approach, Gu et al. used a CNT-template-assisted CVD process with SiO vapor, showing that defect density influenced whether the resulting nanowires behaved as metallic or semiconducting materials [26].

2.1.3. Template-Assisted Growth

Template-guided growth using anodic aluminum oxide (AAO) has proven effective for synthesizing highly oriented SiC nanowire arrays. In one such approach, Li et al. employed a chemical vapor reaction route, where a mixture of Si, $SiO_2$, and $C_3H_6$ vapor reacted within the confined nanopores of an AAO membrane, enabling SiO formation and subsequent growth of β-SiC nanowires along the [111] direction [27]. The AAO matrix introduced spatial confinement, whereby the vertical alignment was achieved and the morphology of the wires was uniform over the large surfaces. In a similar approach, Xi et al. used 1, 10-phenanthroline as a molecular template to cause linear assembly of Si coordination complexes, which allowed formation of ultrathin β-SiC nanowires

 doi:10.20944/preprints202605.0609.v1



through π-stacking and steric hindrance effects [28] . Figure 3 is the growth sequence, in which vapor infiltration, nucleation, and axial expansion within the pores have been schematically presented.

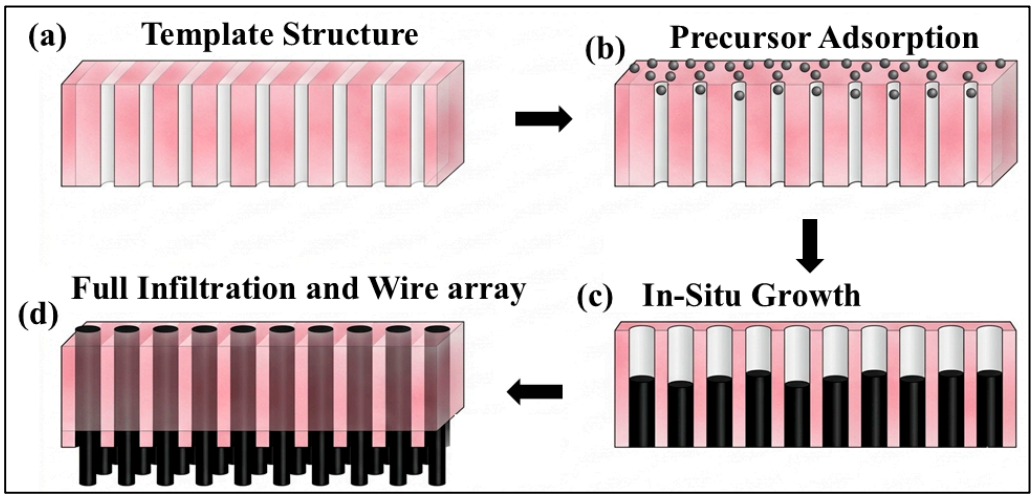


**Figure 3.** Growth process of highly oriented SiC nanowire arrays in a template.

2.1.4. Molten Salt Synthesis (MSS)

The preparation of molten salt has become an affordable and scalable technique in the synthesis of SiC nanowires with relatively moderate conditions. Ding et al. showed that silicon powder was reacted with a carbon template made of phoenix wood in KCl-KF molten salt media in the presence of an argon atmosphere at temperatures between 1250 and 1400 °C. The molten salts were used as a transport medium of silicon species, which allowed them to diffuse into the carbon template and localized silicon species concentration formed through a template-growth process [29]. The overall synthesis scheme is illustrated in Figure 4. A similar molten salt-based electrosynthesis was reported by Zou et al., where SiC nanowires were directly produced from $SiO_2$/C precursors in molten $CaCl_2$ via solid-state electroreduction and dissolution electrodeposition processes, all without requiring templates or catalysts [30].

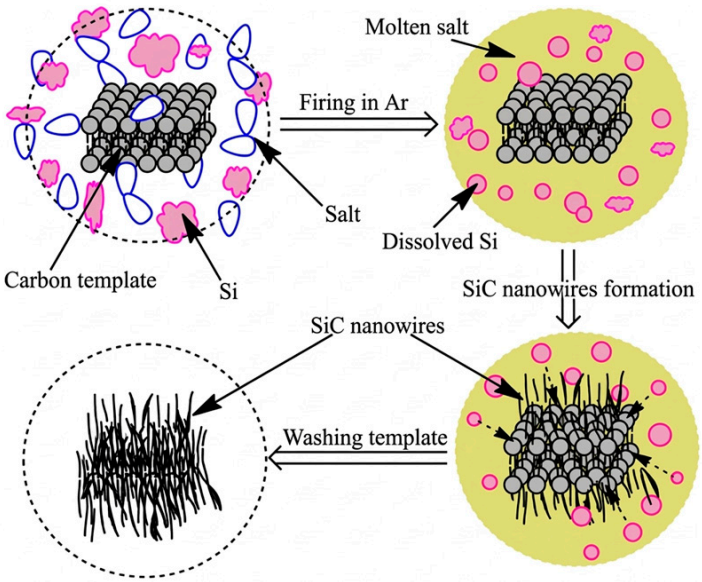


**Figure 4.** Schematic illustration of SiC nanowire **growth** using molten salt synthesis with a carbon template and silicon powder under an argon atmosphere. Reproduced with permission from Ding et al. [29]. © Elsevier.

 doi:10.20944/preprints202605.0609.v1



2.1.5. Laser Ablation

Laser ablation is an effective route for synthesizing SiC nanowires under relatively moderate temperatures and low-pressure conditions. Shi et al. reported the growth of SiC nanowires by irradiating a SiC ceramic target with a KrF excimer pulsed laser in an Ar/$H_2$ atmosphere, with the products deposited on an $Fe(NO_3)_3$ treated graphite substrate at approximately 900 °C [31]. As illustrated in Figure 5, laser irradiation generates a Si/C vapor plume from the SiC target, which is transported to a downstream substrate, where catalyst-assisted nanowire growth occurs. The process follows a VLS mechanism, in which Fe catalyst droplets adsorb vapor species, undergo supersaturation, and subsequently drive the nucleation and elongation of SiC nanowires.

Laser ablation has also been employed to produce a range of one-dimensional Si–C nanostructures. For example, Kokai et al. reported the formation of amorphous SiC nanowires together with carbon nanotubes filled with crystalline SiC nanowires by laser ablation of carbon–silicon targets in high-pressure Ar [32]. These findings indicate that the resulting nanostructures are strongly influenced by both target composition and processing conditions.

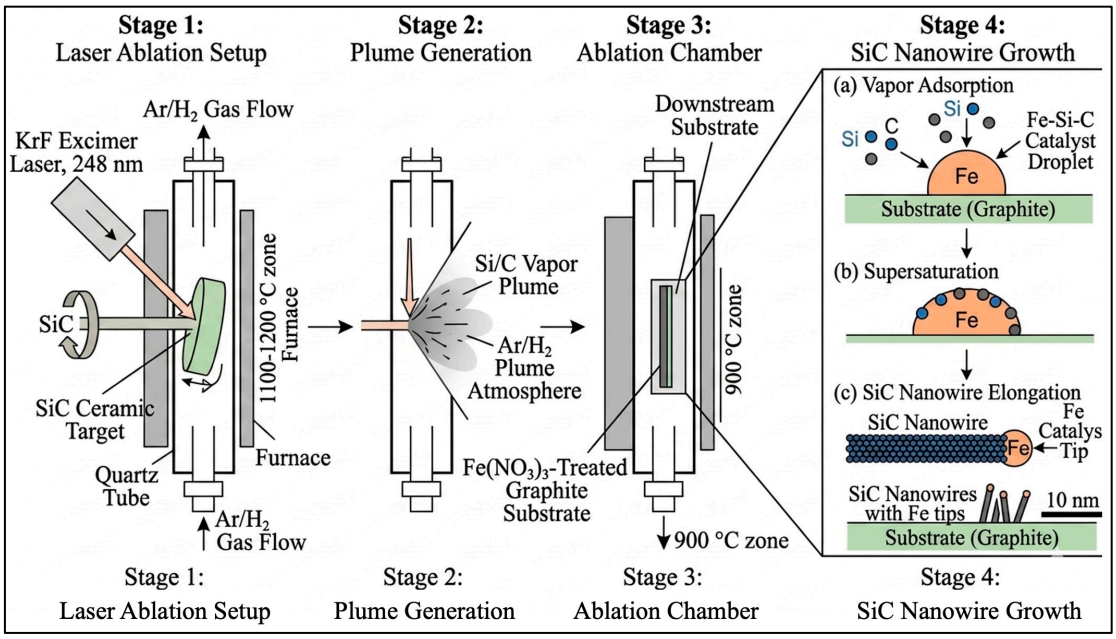


**Figure 5.** Schematic illustration of SiC nanowire growth by laser ablation, showing vapor generation, plume transport, and catalyst-assisted growth on an Fe-treated graphite substrate, based on the mechanism proposed by Shi et al. [31].

2.1.6. Sol-Gel Synthesis

Sol-gel synthesis offers a low cost, scalable and chemically tunable method to prepare SiC nanowires. Li et al. synthesized hexagonal-shaped SiC nanowires by direct heating of a carbonaceous silica gel obtained by a sol-gel procedure [33]. A homogenous mixture of saccharose and tetraethylorthosilicate were aged, dried and pre-treated in this technique to create a carbon rich silica gel. When the nanowires were heated in inert atmosphere, they were formed through vapor solid growth mechanism. The presence of periodic crystal facets of hexagonal shapes on SiC nanoparticles was observed to impact the morphology of the resulting nanowires in a memory effect with their hexagonal cross-sectional shape dictated during growth.

A similar sol gel path was also used by Mishra et al., in which a lignin polysilanol hybrid was pyrolyzed under argon at 1400 °C, and then oxidized. SiC nanowires were produced by the carbothermal reduction of silica using SiO and CO as an intermediate without the use of any external catalysts [34].

 doi:10.20944/preprints202605.0609.v1



A comparison and summary of the raw materials/precursors, preparation processes, growth mechanisms and morphological characteristics of SiC nanowires prepared by different methods is shown in Table 1.

**Table 1.** Comparative summary of major SiC nanowire synthesis methods reported in the literature, including precursor systems, synthesis conditions, growth mechanisms, and resulting morphologies.

| Precursors | Temperature /time /atmosphere | Growth mechanism | Resulting morphology (shape, diameter) | Reference |
|---|---|---|---|---|
| **Carbothermal Reduction** | | | | |
| $SiO_2$ and carbon black; graphite or BN crucible | 1823 K / 4 h / Ar | VS in graphite crucible; not reported for BN crucible | Graphite crucible: uniform nanowires, tens of nanometers BN crucible: chain-beaded nanowires, | [19] |
| $SiO_2$ and carbon black | 1600 °C for 4 h, then 1350 °C for 2 h / Ar | s–s + s–v (1st stage); v–v (2nd stage) | Nanowires, 40–120 nm | [20] |
| FeSi alloy powder and Si powder on graphite plate | 1600 °C / 3 or 6 h / Ar | SLS + VLS | 3 h: curved nanowires 6 h: straight nanorods; ~100 nm | [21] |
| Low-purity $SiO_2$ and carbon black | 1400 °C / 2 h / Ar | VLS | Nanowires, ~60 nm | [22] |
| $\alpha$-SiC powder, polycarbosilane, polyurethane sponge | 1000–1300 °C / 1 h / $N_2$ | VLS at 1000–1100 °C; VS at 1300 °C | 1000 °C: short nanowires with spherical caps 1100 °C: straight/curved nanowires, 50 nm 1300 °C: nanowires without spherical caps, diameter not reported | [23] |
| **Chemical Vapor Deposition** | | | | |
| Si and $SiO_2$ powders; graphite crucible and graphite felt | 1300 °C / 3 h / Air | VS | Core–shell nanowires, ~50 nm | [24] |
| $CH_3SiCl_3$ (MTS), $H_2$, Ar, and C/C substrate | 1050–1150 °C / 2 h / $H_2$–Ar | VS | Nanowires, ~70 nm; after oxidation, coaxial nanocables | [25] |
| Carbon nanotubes and SiO powders | 1300 °C / Not reported / Not reported | Not reported | Defect-rich and nearly perfect single-crystal nanowires, not reported | [26] |

 doi:10.20944/preprints202605.0609.v1



| | | | | |
|---|---|---|---|---|
| **Template-Assisted Growth** | | | | |
| Ball-milled Si and $SiO_2$ powder, $C_3H_6$, AAO template, graphite reaction cell | 1230 °C / 3–5 min / Ar + $C_3H_6$ | Not reported | Highly oriented nanowire arrays, 30–60 nm | [27] |
| $SiCl_4$, $CH_3OCH_2CH_2OCH_3$, Mg, and 1,10-phenanthroline | 650 °C / 6 h / sealed autoclave; $N_2$ glove-box loading | Molecule-template mechanism | Ultrathin nanowires, ~8 nm | [28] |
| **Molten Salt Synthesis** | | | | |
| Phoenix wood-derived carbon template, Si powder, KCl/KF molten salt | 1250–1400 °C / 3 h / Ar | Template-growth mechanism | Nanowires in cellular pores, ~30 nm | [29] |
| $SiO_2$/C precursors in molten $CaCl_2$ | 900 °C / 15 h / molten $CaCl_2$ | Solid-to-solid electroreduction + dissolution-electrodeposition | Homogeneous nanowires, 30–50 nm | [30] |
| **Laser Ablation** | | | | |
| SiC ceramic target; graphite substrate coated with iron nitrate; Ar + 5% $H_2$ | ~900 °C substrate temperature / 2 h / Ar + 5% $H_2$ | VLS | Core–shell nanowires, 59–110 nm | [31] |
| Carbon–silicon targets | Not reported / high-pressure Ar (up to 0.9 MPa) | Not reported | Amorphous SiC nanowires: 5–30 nm, carbon nanotubes filled with crystalline SiC nanowires: 10–60 nm | [32] |
| **Sol-Gel Synthesis** | | | | |
| Tetraethylorthosilicate, ethanol, saccharose solution | 1500 °C / 1 h / Ar | VS | Hexagonal nanowires, 50-100 nm | [33] |
| Kraft lignin and sol-gel derived polysilanol from MTEOS | 1400 °C / 1 h / Ar, followed by oxidation at 800 °C for 1 h | Not reported | Continuous, Y-shaped branched nanowires, 50-200 nm | [34] |

*2.2. Morphology Control*

The morphology of SiC nanowires is strongly dependent on the synthesis conditions [35]. Cheong and Lockman demonstrated that catalyst-free chemical vapor growth could produce 6H-SiC nanostructures with either nanowire or nanoneedle morphologies, depending on the synthesis temperature and crucible height. In their study, the effects of heating temperature (1250, 1300, and 1350 °C) and crucible height (9, 13, and 16 cm) on the formation of nanowires and nanoneedles were systematically investigated [36]. The overall morphology evolution of 6H-SiC nanostructures as a

 doi:10.20944/preprints202605.0609.v1



function of temperature and crucible height is summarized in Figure 6, which provides a general view of how macroscopic growth conditions influence the final nanostructure shape.

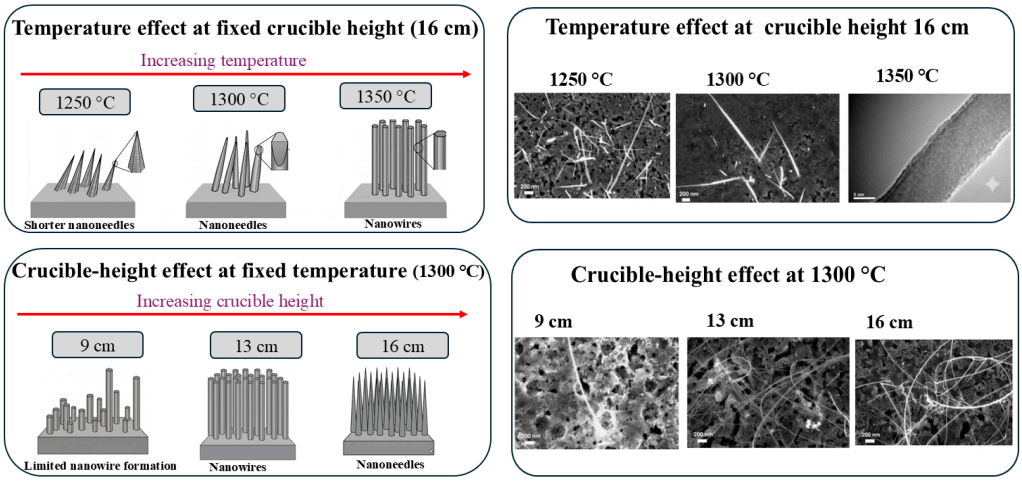


**Figure 6.** Schematic summary and representative SEM/TEM images illustrating the temperature- and crucible-height-dependent morphology evolution of 6H-SiC nanostructures; SEM/TEM images reproduced with permission from Cheong and Lockman. [36]. © Elsevier.

Catalyst-assisted growth provides an3 additional level of morphological control. Guo et al. showed that $Al_2O_3$ and Ni catalyst films produced markedly different morphologies through oxide-assisted growth and VLS growth, respectively. $Al_2O_3$ led to the formation of pearl-chain-like nanowires, whereas Ni favored straight single-crystal nanowires growing along the (111) direction. In addition to catalyst type, catalyst-film thickness also influenced the density, layer thickness, crystallinity, and defect structure of the resulting SiC nanowires [37]. These representative morphology differences are further illustrated in Figure 7a,b, where pearl-chain-like nanowires and straight catalyst-assisted nanowires are shown together with characteristic tip features associated with the growth process.

The factors controlling SiC nanowire morphology can also influence crystallinity and polytype evolution. Lin et al. showed that SiOC intermediates promoted nanowire elongation by supplying oxygen and also regulated phase evolution during growth. With increasing temperature, the nanowires progressively transformed into highly ordered 3C-SiC, reaching complete conversion at 1550 °C, while oxygen-assisted stress relaxation promoted long-range structural ordering [38]. Huang reported that SiC nanowire growth under carbothermal conditions can involve a 2H-to-3C transformation, indicating that crystal structure may evolve during growth rather than being fixed at the nucleation stage [39]. In In a related study, Krishnan et al. demonstrated that the crystallographic orientation of 4H-SiC substrates influences both nanowire growth direction and dominant SiC polytype during epitaxial growth, owing to the substrate-dependent epitaxial relationship at the growth interface [40]. The structural aspect of this evolution is highlighted in Figure 7c,d, where the proposed 2H-to-3C transformation is supported by HRTEM imaging and stacking-sequence analysis, confirming that crystal structure can evolve during growth rather than remaining fixed at the nucleation stage. Taken together, these findings show that morphology, crystallinity, and polytype are often governed by the same growth conditions rather than evolving independently.

 doi:10.20944/preprints202605.0609.v1



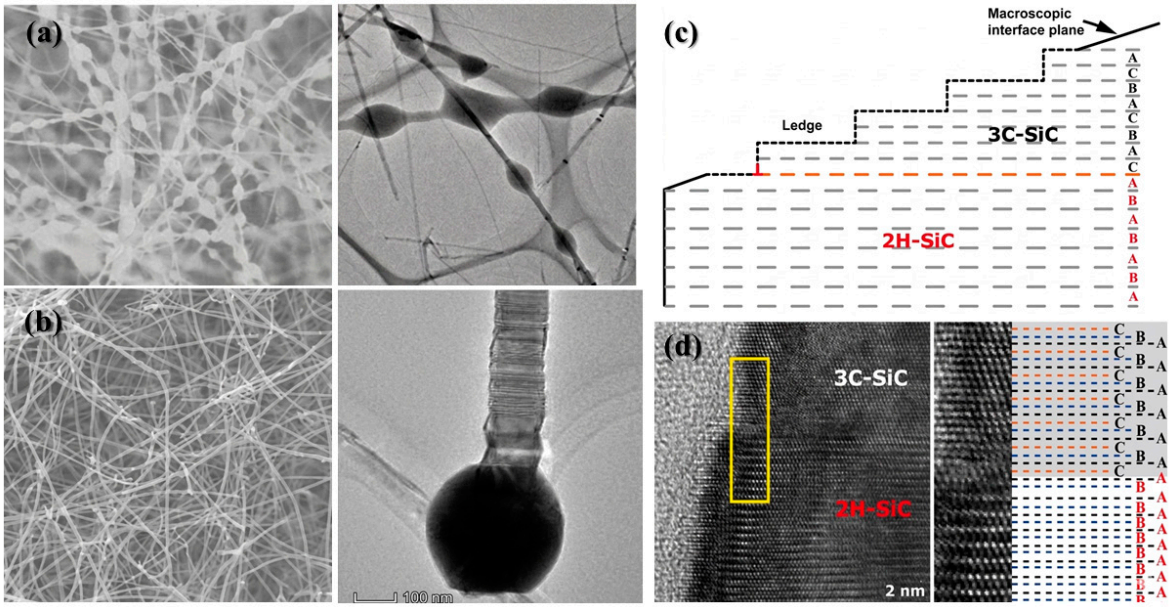


**Figure 7.** Representative morphologies and structural evolution of SiC nanowires. (a) Pearl-chain-like nanowires formed under oxide-assisted growth. (b) Straight nanowires and catalyst-assisted VLS growth with a spherical tip. (c) Schematic illustration of 2H-to-3C polytype transformation during growth. (d) HRTEM image and corresponding stacking sequence showing the coexistence and transition between 2H-SiC and 3C-SiC. Adapted from Refs. [37,39].

### *2.3. Structural and Physicochemical Properties*

#### 2.3.1. Crystallographic and Structural Features

The crystallographic and structural features of SiC nanowires are determined by polytype, preferred growth direction, defect structure, and surface composition. He et al. showed that SiC nanowires can be selectively obtained as 3C-SiC, 2H-SiC, or mixed 3C/2H structures by adjusting the deposition atmosphere, demonstrating that the stacking sequence of SiC nanowires is highly sensitive to growth conditions. This result confirms that one-dimensional SiC does not adopt a single crystallographic form, but can stabilize different polytypes depending on the synthesis environment [41].

The preferred growth direction is also closely related to crystallographic structure and substrate effects. Wang et al. reported that substrate orientation can induce preferred alignment of SiC nanowires, with growth along [$\bar{1}$102] on SiC (0001) substrates and along [10 $\bar{1}$0] on SiC (10 $\bar{1}$0) and (11 $\bar{2}$0) substrates, indicating that crystallographic matching at the growth interface strongly affects nanowire orientation [42]. In addition, Chen et al. showed that SiC/$SiO_2$ core–shell nanowires synthesized at low temperature consisted mainly of single-crystal 3C-SiC together with defective 3C regions along the [111] direction [43]. These studies show that growth orientation is not only polytype-dependent, but also strongly influenced by the interfacial crystallographic relationship during growth.

Defect structures are another important part of the crystallographic description of SiC nanowires. Li et al. reported periodically twinned 6H-SiC nanowires with fluctuating stems, in which alternating high-density stacking faults were associated with axial diameter fluctuation. This finding indicates that twin boundaries and stacking faults are not merely incidental defects, but can contribute directly to local structural modulation during nanowire growth [44].

The presence of a surface oxide film should also be considered when describing the structural features of SiC nanowires. Many reported SiC nanowires are covered by a thin amorphous $SiO_2$ or $SiO_x$ film formed by surface oxidation, resulting in core–shell structures rather than bare single-phase nanowires. Reported SiC/$SiO_2$ and SiC/$SiO_x$ core/shell nanowires confirm that this oxide sheath is a

 doi:10.20944/preprints202605.0609.v1



realistic and structurally significant feature [45,46]. Therefore, the surface oxide film should be regarded as an integral part of the structural description of SiC nanowires

2.3.2. Mechanical Properties

SiC nanowires exhibit excellent mechanical performance, with Young's modulus generally reported in the several-hundred-gigapascal range. Their tensile strength typically increases as the diameter decreases, mainly because thinner nanowires contain fewer critical internal defects. Cheng et al. showed that nanowires with diameters of 17 nm or less could sustain tensile stresses above 25 GPa, approaching the theoretical strength of defect-free 3C-SiC [47]. They further concluded that this size dependence was governed primarily by size-dependent defect density, rather than by a generic surface effect. Wang et al. also reported, from molecular dynamics simulations, that Young's modulus increased from about 520 to 555 GPa as the diameter decreased from 3.3 to 1.6 nm, indicating size-dependent stiffening at very small dimensions [48]. The same study showed that Young's modulus decreased with increasing temperature, reflecting thermally induced lattice softening; these data are summarized in Table 2.

At small diameters, however, surface-related contributions can become more significant because the high surface-to-volume ratio increases the influence of surface stress, surface bonding, and any surface oxide layer on the overall mechanical response. This point is particularly relevant for SiC nanowires because many are not bare crystals, but are covered by a thin $SiO_2$ sheath. Ma et al. showed that the bending Young's modulus of $SiO_2$@SiC nanowires decreased clearly with increasing oxide-shell thickness, and that the influence of the oxide sheath should not be ignored when the shell thickness exceeds about 5 nm. Therefore, the effect of the surface on mechanical behavior should be understood not only in terms of nanoscale surface atoms, but also in terms of the mechanical contribution of the surface oxide layer itself [49].

Defect structure also plays an important role in the mechanical response of SiC nanowires. Perisanu et al. measured the mechanical resonance of individual SiC nanowires and showed that thinner and better-crystallized nanowires exhibited higher stiffness and higher quality factors, indicating better mechanical stability under dynamic loading [50]. These results, together with the tensile and simulation studies above, show that the mechanical properties of SiC nanowires are controlled by a combination of diameter, defect density, temperature, and surface condition.

**Table 2.** Temperature-dependent Young's modulus (GPa) of SiC nanowires with varying diameters, as determined by molecular dynamics simulations (41).

| Diameter (nm) | 300 K | 600k | 900k | 1200k | 1500k |
|---|---|---|---|---|---|
| 1.6 | 555 | 540 | 525 | 510 | 495 |
| 2.4 | 540 | 525 | 510 | 495 | 480 |
| 3.3 | 520 | 505 | 490 | 475 | 460 |

2.3.3. Electrical and Optical Properties

The electrical and optical properties of SiC nanowires are fundamentally governed by the wide indirect band gap of SiC, which underlies their potential for high-temperature electronic devices and short-wavelength optoelectronic applications. Because the band gap depends strongly on polytype, the electronic and optical behavior of SiC nanowires also varies with crystal structure. At room temperature, the band gap is about 2.39 eV for 3C-SiC (β-SiC), 3.02 eV for 6H-SiC, 3.26 eV for 4H-SiC, and 3.33 eV for 2H-SiC. In sufficiently small SiC nanowires, the band gap can become slightly larger than that of bulk 3C-SiC because of quantum-confinement effects [51–53].

For the electrical response, the crystal type should be stated explicitly. Zhou et al. fabricated field-effect transistors based on β-SiC nanowires, that is, cubic 3C-SiC nanowires, and observed n-

 doi:10.20944/preprints202605.0609.v1



type semiconducting behavior with gate-modulated conduction. The reported carrier mobilities were 6.4 and 15.9 $cm^2 V^{-1} s^{-1}$ at Vds = 0.01 and 0.05 V, respectively. These results show that SiC nanowires retain semiconducting transport characteristics at the nanoscale, although the measured response is still influenced by contacts and interface-related scattering [54].

UV–vis absorption and PL measurements confirm that these nanowires possess a bandgap of approximately 2.85 eV and exhibit a strong blue emission at 470 nm (2.64 eV). The slight difference between absorption edge and emission peak reflects a typical Stokes shift, while the broad low-energy tail extending from 480 to 600 nm is attributed to recombination at stacking faults and twin boundaries. This emission behavior is illustrated in Figure 8, which shows the room-temperature photoluminescence spectrum with both the main emission peak and defect-related tail clearly visible [55].

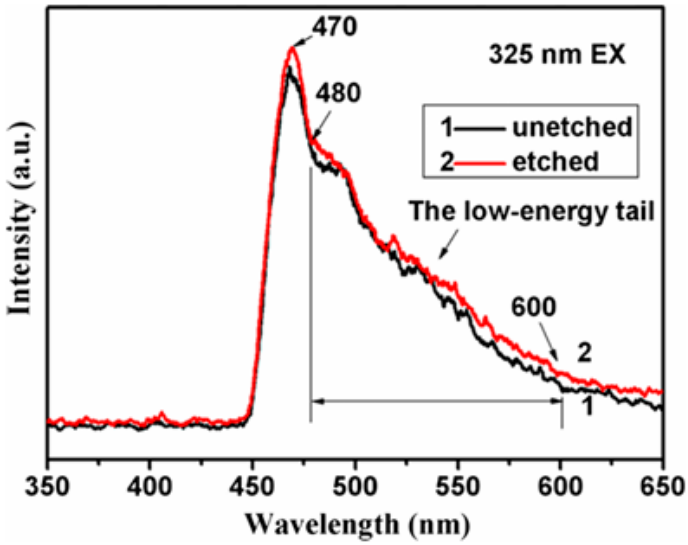


**Figure 8.** PL spectra of unetched and etched 3C–SiC nanowires excited at 325 nm, showing emission at 470 nm and a broad low-energy tail. Reproduced with permission from Chen et al.[55] . Springer Nature.

### 2.3.4. Thermal Properties

SiC nanowires exhibit attractive thermal behavior because they combine high thermal stability with low thermal expansion and size-dependent heat transport. Thermogravimetric analysis has shown that SiC nanowires remain relatively stable in air up to about 1000 °C, whereas oxidation becomes more pronounced above this temperature [56]. In addition, the low coefficient of thermal expansion of SiC is beneficial for dimensional stability and thermal-shock resistance. Sultan et al. reported that the coefficient of thermal expansion of 3C-SiC is about $2.4 \times 10^{-6}$ $°C^{-1}$ at 25 °C, while Hossain et al. showed that thermal expansion in 3C-SiC nanowires becomes diameter dependent because surface and core bonds contribute differently in thinner nanowires [57,58]. Thus, thermal expansion in SiC nanowires is not only an intrinsic lattice property, but also a size-sensitive feature at the nanoscale.

The thermal conductivity of SiC nanowires is, however, much lower than that of bulk SiC because heat transport is strongly limited by phonon scattering at free surfaces, defects, and internal interfaces. Using the 3ω method, Lee et al. measured a thermal conductivity of about 82 ± 6 W $m^{-1}$ $K^{-1}$ for a single β-SiC nanowire, which is far below the value for bulk single-crystal SiC. Valentín et al. further showed that the thermal response of individual β-SiC nanowires is governed by a combination of boundary, impurity, and defect scattering [59,60].

In addition to temperature, thermal conductivity is also sensitive to nanowire geometry and structural disorder. Termentzidis et al. showed that diameter or polytype modulation introduces additional thermal resistance, while Yin et al. reported clear size and interface effects on heat transport in 3C/4H-SiC nanowires [61,62]. Overall, the spread of reported thermal-conductivity

 doi:10.20944/preprints202605.0609.v1



values in SiC nanowires can be understood in terms of differences in diameter, crystallinity, defect density, surface roughness, and internal interfaces.

### *2.4. Limitations of SiC Nanowires*

Despite their excellent thermal stability, high mechanical strength, and chemical resistance, pristine SiC nanowires still exhibit several intrinsic limitations that restrict their direct use in advanced functional systems. A key limitation is their relatively inert surface chemistry, which provides only limited electrochemically active sites for interfacial redox processes. Consequently, bare SiC nanowires generally exhibit modest electrochemical performance and usually require surface modification or coupling with electroactive phases to achieve competitive performance in supercapacitors, sensors, and related devices [63,64].

Another important limitation stems from microstructural and interfacial considerations. SiC nanowires commonly contain crystallographic defects, including stacking faults and related structural irregularities, and these features can affect charge transport, local mechanical reliability, and performance consistency. In addition, when integrated into metals, oxides, carbon matrices, or polymers, SiC nanowires often require deliberate interface design to ensure efficient stress transfer and low-resistance interfacial contact. Without such optimization, interfacial debonding and inefficient load or charge transfer can become important constraints [11].

More broadly, pristine SiC nanowires are primarily valued for structural robustness and environmental stability rather than for strong intrinsic catalytic, pseudocapacitive, or multifunctional interfacial activity. This limits their effectiveness in integrated systems that demand simultaneous mechanical durability, electrochemical responsiveness, and tunable surface functionality. As a result, recent research has increasingly shifted from bare SiC nanowires toward coated, doped, and hybrid architectures, in which the SiC core serves as a stable structural framework while the secondary phase provides the missing functional activity [65].

## 3. Coating Strategies for SiC Nanowires

### *3.1. Rationale for Surface Coating*

SiC nanowires can be made more chemically durable, structurally resilient, functionally versatile, and interfacially compatible by applying surface coatings. To fully utilise SiC nanowires in cutting-edge technological applications these alterations tend to be essential.

#### 3.1.1. Chemical Protection: Oxidation and Corrosion Resistance

Although SiC nanowires are known for their outstanding thermal and chemical stability, their surfaces may still undergo oxidation under prolonged exposure to high-temperature oxidizing environments. Surface coating provides an effective means of suppressing such degradation by forming a barrier layer that limits the diffusion of oxygen and other reactive species. The oxidation of SiC can be expressed as follows in equation 4.

$$\mathrm{SiC(s) + 2O_2(g) \rightarrow SiO_2\ (s) + CO_2(g)} \quad (4)$$

$$\Delta_r G^{\theta} = (0.1688T - 1231.37)\ \mathrm{kJ \cdot mol^{-1}}$$

where T is the absolute temperature in K. The negative $\Delta_r G^{\theta}$ values indicate that SiC oxidation is thermodynamically favorable [66]. Therefore, the role of surface coating is not to alter the thermodynamic tendency of oxidation, but rather to retard the reaction kinetically by blocking oxygen ingress and stabilizing the surface. Ceramic or oxide coatings are especially effective in this regard, as they can reduce active surface reactions and improve the long-term oxidation and corrosion resistance of SiC nanowires under chemically aggressive and high-temperature conditions [67,68].

 doi:10.20944/preprints202605.0609.v1



3.1.2. Structural Reinforcement

Stability of the structure is a major reason why coatings are applied to SiC nanowires, particularly when they are incorporated in multilayer or composite materials. As depicted by Zhang et al., the presence of coating alleviates stress along the interface between the nanowires and the surrounding matrix and this decreases the probability of cracking or separation due to the difference in thermal expansions [69]. These coating also increase the adhering performance of the nanowires to the other layers leading to higher strengths and stability. Lu et al. suggest that the surface-treated nanowires are beneficial as they avoid the damage over time as they are more firmly bonded within the system of repetitive heating and stressed systems [70]. Surface coatings, in this manner, facilitate the mechanical reliability of the SiC nanowire-based structures besides providing chemical protection.

3.1.3. Functional Enhancement

Surface coating is mandatory in improving the functional behaviour of SiC nanowires particularly in electronic and sensing applications. In a study of surface physics, and nanowire interfaces, it has been established that surface passivation in semiconducting nanowires inhibits defect states, carrier mobility, and increases electronic reliability [71]. The same objective is achieved in coating SiC nanowires to increase homogeneity of the surfaces and reduce charge traps.

The importance of surface modification in practical uses was also emphasized in a research on SiC@C core-shell nanowires where a coating made of carbon was found capable of modifying the underlying SiC dielectric environment and surface charge behaviour [72]. These advancements make better compatibility in devices such as sensors and field emitters, better distribution of electric fields, and consistent transmission of charges possible. Consequently, to maximally use SiC nanowires in more advanced electronic and optoelectronic systems, surface coatings are required.

3.1.4. Interfacial Engineering and Compatibility

Surface coating of SiC nanowires is significant in enhancing the compatibility of surfaces with the surrounding materials. Uncoated nanowires can have a low chemical interaction and low surface wettability that can result in weak bonding and the development of interfaces. Coatings are used to overcome these difficulties by changing the energy of the surfaces and adding functional groups to enhance high adhesion. This allows improved dispersion and contact at the interface which is particularly useful in multi-phase systems. Research on SiC nanowires used in conjunction with other active materials has indicated that surface modified nanowires have a better interfacial integration which minimizes the mismatch at the boundaries and facilitates a stable assembly [73].

*3.2. Coating Methods for SiC Nanowires*

3.2.1. Wet Chemical Method

Wet chemical technique involves reactions in atmospheric pressure with ambient or slightly heated solutions. They are the most common methods to add catalytic or functional nanoparticles on SiC nanowires and are simple and scalable.

As an indication, Wang et al. utilized a photodeposition technique to coat platinum nanoparticles on β-SiC nanowires by subjecting an $H_2PtCl_6$ solution to the UV light [74]. This technique made the core of nanowires suitable in photocatalytic use since it enabled homogenous loading of Pt without destroying it. The method is particularly useful in deposition of noble metals or metal oxides on the surface of nanowires by controlled reduction or adsorption of ions.

3.2.2. Hydrothermal Method

Hydrothermal synthesis is a method that produces uniform and crystalline coatings on nanowires by reactions in high-temperature and pressure sealed autoclaves. This is especially suited for forming heterojunctions.

 doi:10.20944/preprints202605.0609.v1



A representative example is the CdS-coated SiC nanowire system reported by Peng et al., where the formation of the heterostructure is closely associated with lattice matching between CdS and the SiC substrate. In such systems, reduced lattice mismatch facilitates coherent nucleation and growth of the secondary phase, leading to improved interfacial contact and more efficient charge transfer across the heterojunction. In this approach, SiC nanowires act as structural templates, onto which $Cd^{2+}$ species are first adsorbed through electrostatic interaction. Subsequent hydrothermal sulphuration converts these surface-bound precursor species into CdS nuclei, which then grow into a conformal coating. Because nucleation occurs at the nanowire surface rather than in the bulk solution, this process promotes uniform coverage and enhances the structural integrity of the SiC/CdS interface [75]. The mechanism illustrated in Figure 9, further highlights the role of hydrothermal conditions in regulating coating structure and phase evolution. Initially, $Cd^{2+}$ ions are adsorbed onto the SiC surface, forming a precursor layer via electrostatic attraction. Upon sulfur incorporation, CdS nuclei precipitate and subsequently grow on the nanowire surface. Importantly, the hydrothermal temperature governs the crystalline phase and morphology of the deposited CdS: at 60 °C, primarily cubic CdS (C-60) is obtained; at 160 °C, a mixed cubic/hexagonal phase (CH-160) forms; and at 220 °C, the structure evolves toward predominantly hexagonal CdS (H-220). This temperature-dependent phase evolution reflects differences in nucleation and growth kinetics, which in turn influence interfacial crystallinity and lattice compatibility. Therefore, the hydrothermal method not only enables coating deposition but also provides a means to tailor interfacial crystallography, which is critical for optimizing charge separation and photocatalytic performance.

In related work, Liao et al. synthesized $SnO_2$/SiC nanowire heterostructures via a solvothermal process in ethanol. Since this method employs a non-aqueous solvent, it is more appropriately discussed in a separate solvothermal subsection rather than within the hydrothermal framework [73].

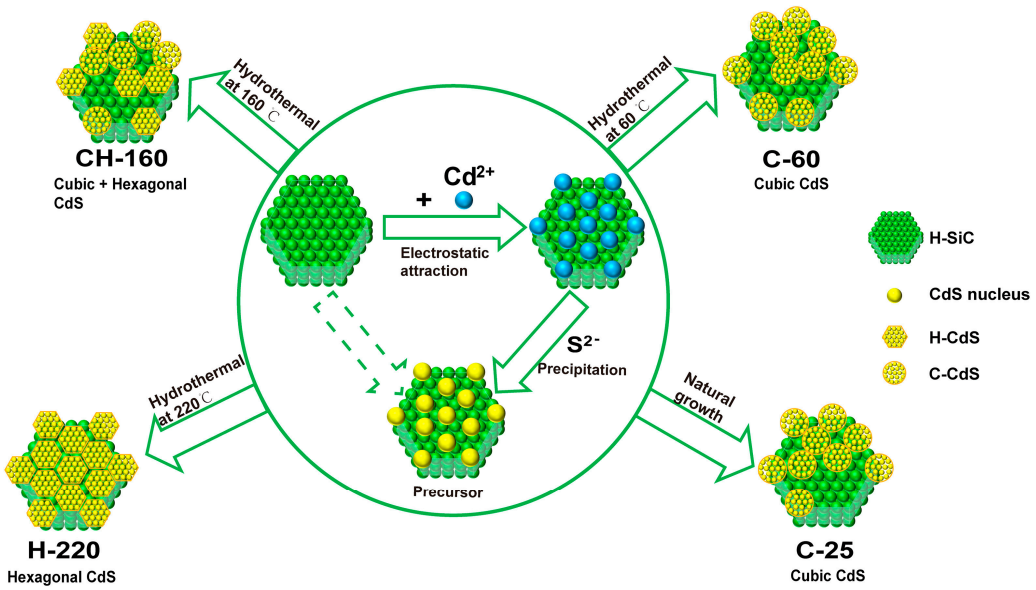


**Figure 9.** Hydrothermal synthesis of CdS-coated SiC nanowires via $Cd^{2+}$ adsorption followed by sulphidation. Reproduced with permission from [73]. © Elsevier.

### 3.2.3. Thermally Induced Coating

Thermally induced coating methods enable the formation of surface layers on SiC nanowires through direct heat-driven transformation of precursor compounds. These approaches include both functional heterostructures formed via thermal polymerization and nanoscale surface layers engineered during high-temperature synthesis.

Wang et al. achieved a uniform g-$C_3N_4$ coating on SiC nanowires by pyrolyzing thiourea at 550 °C in a nitrogen atmosphere, forming a tightly bound Z-scheme heterojunction suitable for visible-light photocatalysis [76]. In a separate study, Yang et al. synthesized single-crystal SiC

 doi:10.20944/preprints202605.0609.v1



nanowires with a conformal carbon coating, developed during the thermal processing of a polymer-derived ceramic precursor [77]. This carbon layer enhanced the nanowires' mechanical reinforcement capability when embedded in ceramic matrices, contributing to improved strength and toughness in composite systems.

### 3.2.4. Chemical Vapor Deposition Method

Chemical vapor deposition (CVD) is a general, gas-phase technique that can be employed in depositing conformal coating onto SiC nanowires by reacting volatile species at high temperatures. In the case of advanced nanowires applications this process provides specific control of the growth environment and aids in the formation of compositionally stable homogeneous coats.

Tang et al. produced SiC nanowires with uniform boron nitride (BN) coatings with a high temperature CVD method in the presence of $BCl_3$ and $NH_3$ [78]. Consistent core–shell morphology with smooth and continuous BN coverage was shown by the resulting BN@SiC nanostructures. This technique focuses on the ability of CVD to form chemically inert layers to enhance the environmental stability of SiC nanowires.

In a similar work, Chu et al. developed SiC nanowire-based coating on carbon-carbon (C/C) materials through a two-step CVD method [79]. The initial stage involved the in-situ growth of SiC nanowires on the surface of the composite followed by a dense deposition of SiC. This two-step process demonstrates that CVD is versatile in the sense that it can be used to combine a surface coating and nanowires synthesis into one solid and unified system.

### 3.2.5. Precursor Infiltration and Pyrolysis

Precursor Infiltration and Pyrolysis (PIP) has been found to be a useful approach in coating SiC nanowires, especially where thermal stability in further high-temperature treatment is important.

A dual layer coating technique was used in a study by Xie et al. to safeguard the SiC nanowires against structural damage as they were exposed to silicon-rich environments at high temperatures. First, plasma-enhanced chemical vapor deposition (PECVD) was used to coat the surface of the nanowires with a carbon layer, to create a vertically oriented graphene (VG) structure that acted as an interlayer to provide thermal resistance. This was followed by the application of a SiC outer shell via the PIP method, wherein a polycarbosilane precursor was infiltrated into the nanowire network under pressure and subsequently pyrolyzed under vacuum at high temperature. Multiple cycles of infiltration and pyrolysis yielded a conformal SiC coating that encapsulated the nanowires. This dual-layer architecture effectively maintained the nanowire morphology during subsequent processing at 2173 K, thereby preserving their one-dimensional structure and reinforcing capability within the composite system [80]. A schematic overview of this multi-step coating process is shown in Figure 10.

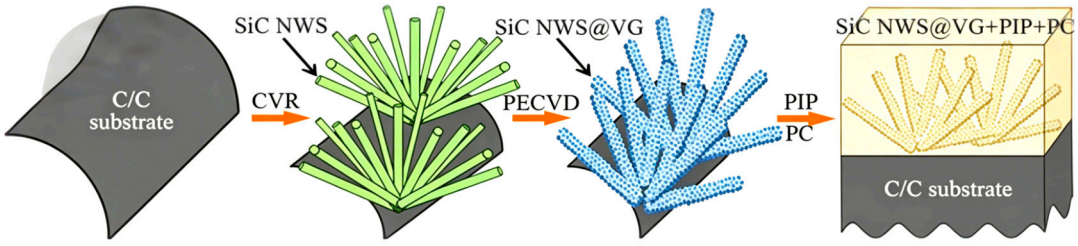


**Figure 10.** Schematic illustration of the coating process for SiC nanowires using PECVD and PIP methods prior to pack cementation. Reproduced with permission from Xie et al. [80] © Elsevier.

### 3.2.6. Atomic Layer Deposition Method

Atomic layer deposition (ALD) offers precise, layer-by-layer control for coating SiC nanowires with uniform and conformal thin films. Its self-limiting surface reactions make it ideal for high-aspect-ratio structures.

 doi:10.20944/preprints202605.0609.v1



Tak and Yong used plasma-enhanced ALD to deposit $ZrO_2$ coatings on SiC nanowires at 150 °C using zirconium tertiary butoxide and hydrogen plasma [81]. The coating thickness was tunable by cycle count, and post-annealing at 900 °C yielded a polycrystalline $ZrO_2$ shell. The resulting $ZrO_2$@SiC structures exhibited improved surface stability and are suitable for dielectric and sensor applications.

### *3.3. Effect of Coating Parameters*

#### 3.3.1. Thickness

The aspect ratio of surface coating of SiC nanowires is a determining factor in the regulation of structural and functional characteristics. This parameter should be optimized because the low and excessive coating thickness may cause performance to decrease. As much as ultra-thin layers cannot provide sufficient passivation or environmental protection, excessive thick layers can cause interfacial stress, inhibit charge transfer, and reduce mechanical stability.

In research by Chen et al., SiC/$SiO_2$ core shell nanowires were produced through ferrocene-based CVD synthesis, where silica shells were developed that increased the intensity of photoluminescence. The authors stressed that the oxide shell thickness needed to be strictly controlled to prevent the introduction of non-radiative recombination mechanisms and optical transparency with the best results found at intermediate shell thicknesses [43].

Similarly, Ma et al. managed the thickness of the $SiO_2$ shell on the SiC nanowires in a systematical manner by means of an NaOH based post-treatment. Mechanical examination showed that with further increase in shell thickness the bending modulus gradually decreased due to a higher structural compliance and redistribution of stresses across the core-shell boundary. It is important to note that the mechanical trade-offs were important above the shell thickness of approximately 10-14 nm [82]. These results all highlight the fact that accurate regulation of the coating thickness is critical to the preservation of desirable balance between passivation, optical activity and mechanical strength of the SiC nanowire systems.

#### 3.3.2. Uniformity

The uniformity of surface coatings of the SiC nanowires is a crucial parameter that determines interfaces stability, electronic homogeneity, and device stability. Non-uniform layers with discontinuities, spotty coverage, or thickness variations may cause uneven electrical and optical functionality, focal degradation, and decreased protection in severe conditions.

Hu et al. described the synthesis of core shell nanowires of SiC/$SiO_2$ using a thermal evaporation technique in the presence of catalysts. The experiment revealed that synthesis parameters, namely the choice of catalyst, growth temperature and vapour distribution had a considerable influence on the homogeneity of the silica shell. An ideal scenario was the development of a conformal and continuous layer of $SiO_2$ over the entire length of the nanowires. Recently, it was shown that this homogeneous shell structure can improve chemical stability and ensures consistent functional behaviour particularly in high-temperature conditions, or surface-sensitive treatments [83]. Similarly, Liu et al. demonstrated that completely covered $SiO_2$ shells on SiC nanowires were obtainable through catalyst-free thermal evaporation, and complete coverage of the entire surface resulted in enhanced oxidation resistance [84]. These results indicate that deposition parameters have to be controlled to achieve uniform coatings on the SiC nanowires that are required to be integrated into their stability into advanced nanodevices and functional composites.

#### 3.3.3. Adhesion

The adhesion between surface coating and SiC nanowires is important to structural stability under thermal cycling in particular. Although experimental evidence on coated SiC nanowires is scarce, theoretical descriptions and theoretical findings provide valuable new insight on the mechanisms of interfacial adhesion.

By means of a $TaB_2$-SiC system, Zhuang et al. showed that adding pyrolytic carbon-coated SiC nanowires (SiC@PyC) produced a zigzag interlocking interface that greatly improved adhesion and

 doi:10.20944/preprints202605.0609.v1



thermal shock resistance. This interfacial design focuses on the necessity of interface engineering in adhesion performance due to the effective delamination reduction in high-temperature cycling [85]. Emphasizing the vital role of surface topography in promoting interfacial integrity, Zhang et al. also found that roughened SiC inner layers enhanced bonding strength and ablation resistance in $ZrB_2$–SiC coatings on C/C substrates [69]. Complementing these, Morresi et al. demonstrated via multiscale modelling that atomic termination and bonding environment directly affect interfacial bonding in SiC/$SiO_x$ nanowires, so influencing adhesion behaviour [86]. Although direct adhesion tests on coated SiC nanowires remain confined, these results validate structural interlocking and surface engineering as successful techniques for improving coating adhesion in nanowire-based systems.

#### 3.3.4. Compatibility

Compatibility between the coating and the SiC nanowire is a key parameter governing coating stability and long-term performance. In coated SiC nanowire systems, this compatibility can be understood from two closely related aspects: lattice matching and thermal expansion coefficient matching. If either is poorly controlled, internal stress can accumulate during processing or service, increasing the likelihood of cracking, delamination, and gradual performance degradation.

The first aspect is lattice matching. Ferrand and Cibert showed, through continuum elasticity analysis of crystalline core-shell nanowires, that the strain state induced by lattice mismatch is strongly influenced by shell thickness, crystallographic orientation, crystal anisotropy, and differences in stiffness constants between the core and shell. Likewise, Krasnitckii et al. demonstrated that, in composite nanowires with polygonal cores, misfit stress and elastic energy are also highly sensitive to interface geometry and mismatch conditions. These studies indicate that good lattice correspondence and coherent interfacial structure are important for suppressing localized stress concentration and maintaining the structural integrity of coated nanowire systems [87,88].

The second aspect is thermal expansion coefficient matching. Even when a coating exhibits good initial adhesion, differences in thermal expansion behavior between the coating and the SiC nanowire can generate significant thermal stresses during heating and cooling. Under repeated thermal cycling, such mismatch may progressively damage the interface and eventually lead to cracking or delamination. A related example has been reported for SiC-coated PIP-C/SiC composites, where the interface was partially destroyed during thermal shock because of thermal expansion mismatch, illustrating the broader importance of thermal-expansion compatibility for preserving interfacial stability under fluctuating temperature conditions [89].

Taken together, these findings show that compatibility in coated SiC nanowire systems should not be assessed solely in terms of chemical adhesion. Instead, it should be evaluated through a combined consideration of lattice correspondence, interface geometry, elastic matching, and thermal expansion behavior. Achieving this balance is essential for reducing residual stress and ensuring the long-term reliability of coated SiC nanowires.

### *3.4. Structural and Functional Modifications Induced by Coating*

Direct surface coatings applied to SiC nanowires can cause appreciable changes in their structural and functional behaviour, according to recent experimental studies including optical modulation, surface electronic tuning, and improved environmental stability.

$TiO_2$ nanotube arrays synthesized onto SiC nanowire frameworks via hydrothermal processing have been shown to improve corrosion resistance and electrical conductivity, suggesting interfacial modifications that influence surface charge distribution and perhaps shift band-edge positions [90]. In another work, ninefold increase in mid-infrared light absorption was obtained by means of multilayer graphene shells deposited onto SiC nanowires. This enhancement is attributed to strong coupling between the shell's electronic states and the core structure, indicating significant coating-induced modification of the nanowire's optical response [91].Additionally, the deposition of laser-induced graphene/carbon composite shells on SiC nanowires has been reported to improve oxidation resistance under high-temperature conditions. The conformal carbon layers served as thermal

 doi:10.20944/preprints202605.0609.v1



barriers and still retained the crystalline integrity, which strongly improved the mechanical stability and durability of coated nanowire system [92].

Such findings highlight the significance of surface coating as passive protective layers and active modulators of functional behavior in SiC nanowires. Despite the limited research, available evidence supports that well-designed coating can have a significant impact on physical and chemical behavior of SiC nanowire-based materials, which creates a base to further targeted investigations. The main coating routes reported for SiC nanowires are compared in Table 3.

**Table 3.** Representative coating methods for SiC nanowires, including coating materials, key precursors, deposition mechanisms, coating characteristics, and interface features.

| Coating method | Coating material | Key precursors | Deposition mechanism | Coating characteristics | Interface features |
|---|---|---|---|---|---|
| **Wet chemical (photodeposition)** | Pt | $H_2PtCl_6$ solution; UV irradiation | Photoreduction | Uniform nanoparticle decoration | Metal/semiconductor contact |
| **Hydrothermal** | CdS | $Cd^{2+}$ adsorption; sulphidation; 60–220 °C | In situ nucleation and growth | Conformal coating; phase-tunable | Semiconductor heterojunction; lattice-match dependent |
| **Solvothermal** | $SnO_2$ | Sn precursor; ethanol medium | Solution-phase deposition | Uniform oxide coating | Oxide/semiconductor heterojunction |
| **Thermally induced coating** | g-$C_3N_4$ | Thiourea pyrolysis; ~550 °C; $N_2$ | Thermal polymerization | Continuous thin coating | Z-scheme heterojunction |
| **Thermally induced coating** | C | Polymer-derived precursor | In situ carbonization | Conformal carbon shell | Conductive core–shell interface |
| **Chemical vapor deposition (CVD)** | BN | $BCl_3$ + $NH_3$; high temperature | Gas-phase reaction and deposition | Smooth, continuous coating | Ceramic core–shell interface |
| **Chemical vapor deposition (CVD)** | SiC | Two-step CVD on C/C substrate | In situ growth + deposition | Dense outer SiC layer | Strong interfacial bonding |
| **PECVD + PIP** | C (inner) + SiC (outer) | PECVD carbon layer; polycarbosilane infiltration; pyrolysis (~2173 K) | Multi-step infiltration and pyrolysis | Dual-layer conformal coating | Multilayer protective interface |

## 4. Heterojunctions and Interface Engineering

### *4.1. Heterojunction Interfaces in SiC Nanowires*

Heterojunctions are interfaces between two dissimilar substances with different electronic band structures. These junctions ensure charge separation and band alignment via conduction/valence band offset, band bending or depletion region formation.

In the case of SiC nanowires, heterojunctions can be used to both (1) design electronic properties through band alignment, and (2) convert SiC nanowires into multifunctional structures (e.g. SiC/$TiO_2$, SiC/$SnO_2$, SiC/HPW composites). As an example, $SnO_2$-coated SiC nanowires have been shown to have enhanced photocatalytic capability, with a good separation of the charges at the heterointerface [73]. Likewise, photoactive systems of the phosphotungstic acid impregnated SiC nanowire have enhanced photoactivity, which is led by the interaction of the SiC coating of the interface [93].

The relative alignment of conduction and valence bands at the interface between two materials is the ultimate basis of classification of heterojunctions. Such band alignment controls the action of

 doi:10.20944/preprints202605.0609.v1



photogenerated charge carriers, affecting charge separation efficiency, recombination dynamics, and interfacial electric fields. Three major heterojunction designs are of special concern in SiC nanowire-based systems, i.e., Type II (staggered gap), Z-scheme and Schottky junctions. As to Type I (straddling gap), whose conduction band minimum and valence band maximum are positioned within the bandgap of the adjacent material, no experimental realization has yet been reported in SiC nanowire system so far.

#### 4.1.1. Type II Heterojunction

In type II alignment, staggered energy levels are present, in which the conduction band minimum of one material is lower than that of the other, and the valence band maximum is higher. Such asymmetric structure is conducive to spatial segregation of photogenerated charge carriers along the interface of the electrons conducting between components and holes concentrating in one of the components. This arrangement is beneficial in systems where there is the need to suppress the electron-hole recombination and better transfer of charges.

This has been evidenced by several SiC-based hybrid systems. One such case is the g-$C_3N_4$/SiC nanowire heterojunctions, in which the photogenerated electrons in the g-$C_3N_4$ are moved to the conduction band of SiC, and holes are retained in the g-$C_3N_4$ valence band [76]. The separation allows better redox potential and visible-light-driven photocatalytic activity, especially in hydrogen evolution reaction. This effect of band alignment is schematically shown in Figure 11a. Such findings indicate the ability of Type II heterojunctions to maximize interfacial carrier dynamics in photocatalysts based on SiC nanowires.

#### 4.1.2. Schottky Junction

A Schottky junction forms when a semiconductor comes into contact with a metal or semimetal. In SiC-based systems, graphene is an attractive Schottky contact because its work function differs from that of 4H-SiC and can therefore create an interfacial built-in electric field. This field is important because it allows carrier separation to occur without relying on an external bias, which is especially beneficial for low-power photodetection.

A representative example is the graphene/4H-SiC nanowire array ultraviolet photodetector reported by Li et al. In this device, graphene serves as the Schottky contact layer, whereas Ni functions as the external metal electrode for carrier collection. The device exhibited self-powered ultraviolet detection together with fast response and low dark current, showing that Schottky interface engineering can effectively improve the photoresponse of SiC nanowire-based optoelectronic devices [94]. As shown in Figure 11c, the Schottky junction is formed specifically at the graphene/4H-SiC interface. Once contact is established, band bending develops on the 4H-SiC side and a depletion region is created near the interface. Under ultraviolet illumination, electron-hole pairs are generated in the 4H-SiC nanowire region, and the built-in electric field drives their separation and transport in opposite directions. This interfacial design not only suppresses carrier recombination, but also enables self-powered operation with low dark current. Therefore, the significance of the graphene/4H-SiC Schottky junction lies not merely in forming an electrical contact, but in providing an efficient route for regulating carrier dynamics and enhancing ultraviolet photodetection performance.

 doi:10.20944/preprints202605.0609.v1



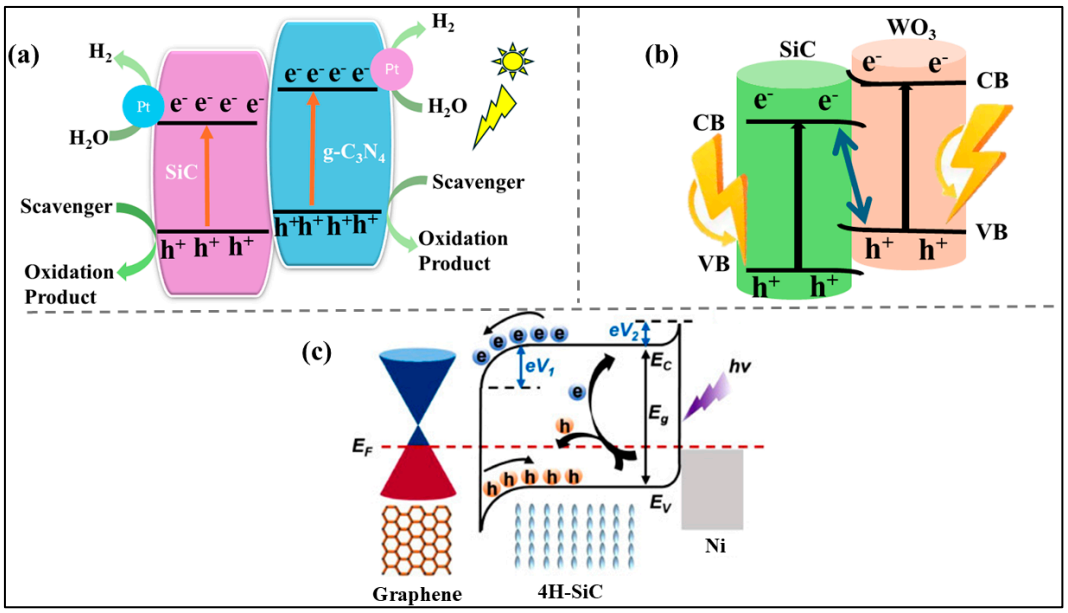


**Figure 11.** Schematic band diagrams of SiC-based heterojunctions: (a) Type II g-$C_3N_4$/SiC, (b) direct Z-scheme $WO_3$/SiC, and (c) graphene/4H-SiC Schottky junction. Panel (c) reproduced with permission from Li et al. [94] © Elsevier.

4.1.3. Z-Scheme Heterojunction

Z-scheme heterojunctions are designed in a way that the directional charge separation is enhanced without limiting the strong redox potentials of the photogenerated carriers. The Z-scheme designs, in contrast to traditional Type II systems, do not have to trade off carrier energy to bidirectional migration, and instead enable selective recombination of low-energy carriers at the interface. The mechanism allows high-energy electrons and holes to be retained in their respective semiconductors that promote increased redox activity in photocatalysis, photoelectrochemical systems, and other energy conversion systems.

Upon such system is the $WO_3$/SiC Z- scheme system where $WO_3$ is the reductive element, and SiC is the oxidative semiconductor. On illumination, the conduction band electrons in SiC will recombine with holes in the valence band of $WO_3$, and the remaining charge carriers will have enough energy to undergo redox reactions. The photoluminescence quenching and energy band analysis both prove that this arrangement enhances efficiency in generating hydrogen and charge separation [95]. The visually represented band lineages and migration of charge in this system are represented in Figure 11b, as such emphasizing the selective interfacial recombination and conservation of high-energy carrier's peculiar to Z-scheme behaviour. This system involves bulk SiC but the principle of charge transfer can still be applied to nanowire designs. SiC has very deep valence and high stability, thereby it is a good candidate in next Z-schemes heterojunction configurations.

In conclusion, internal electric fields, band bending, and energy level alignment between constituent materials define interfacial charge behavior in SiC nanowire heterojunctions. Essential for optimizing photocatalytic and optoelectronic responses, these effects control the efficiency of charge separation and transfer across the junction. SiC nanowires' one-dimensional geometry and high aspect ratio improve interfacial effects even more by promoting anisotropic carrier mobility and strong surface to volume interactions.

These systems highlight how interfacial electric fields and energy-level offsets dictate charge transport behavior. The inherent chemical stability and wide bandgap of SiC nanowires make them especially suited for developing high-performance heterojunctions with controllable carrier dynamics and tunable optoelectronic response.

The conduction band offset in g-$C_3N_4$/SiC nanowire hybrid systems allow photogenerated holes to stay in g-$C_3N_4$ while facilitating electron migration from g-$C_3N_4$ to SiC. Interfacial band bending assists in this charge separation, which is strengthened by impedance spectroscopy and

 doi:10.20944/preprints202605.0609.v1



photoluminescence suppression, both of which show decreased recombination and increased photocatalytic efficiency [76]. Selective interfacial recombination between electrons in SiC and holes in $WO_3$ allows strong redox potential to be maintained in $WO_3$/SiC Z-scheme heterojunctions. This directional charge movement is aided by the interfacial band bending and it has been demonstrated to increase photocatalytic hydrogen evolution in visible light [95].

### *4.2. Interface-Controlled Functional Behavior*

The interface between SiC nanowires and coating materials plays a critical role in determining band alignment, chemical reactivity, and charge transfer behavior. These interfacial effects significantly enhance the functional performance of coated SiC nanowires in electronic devices, sensing, and catalysis. In addition to improving charge separation and mobility, interface engineering also modifies surface interactions and adsorption dynamics, which are essential for multifunctional applications [11].

#### 4.2.1. Interface-Driven Sensing Mechanisms

Interface-induced modulation of the electronic and surface states of SiC nanowires is crucial for gas sensing performance, particularly in terms of sensitivity and selectivity. Surface decoration or coating can alter carrier density and interfacial charge transfer upon gas adsorption, leading to measurable resistance changes. For example, Pt-decorated SiC nanowires have been reported to exhibit enhanced hydrogen sensing performance due to catalytic dissociation and improved interfacial charge transfer [96]. This response is typically governed by band bending or Schottky barrier modulation at the interface. In addition, interfacial defects and surface dipoles introduce additional adsorption sites, further improving response time and sensitivity.

#### 4.2.2. Catalytic Enhancement via Interface Engineering

Adjusting interfacial properties through catalytic coatings can significantly enhance the catalytic activity of SiC nanowires. Coupling with transition metals promotes spillover effects and enhances electron delocalization across the interface, thereby accelerating redox reactions. For example, Ni-coated β-SiC nanowires exhibited a photocurrent density of −32.4 mA $cm^{-2}$ at 1.4 V versus Ag/AgCl, which was attributed to efficient interfacial charge transfer and reduced recombination at the Ni–SiC interface [97]. A similar enhancement has also been reported for Pt-decorated SiC nanowires in photocatalytic hydrogen production [74]. These findings show that catalytic interface engineering can strongly improve carrier utilization and reaction kinetics.

#### 4.2.3. Electronic Behavior Modulation Through Interface Design

Band alignment at the interface strongly influences the electronic properties of SiC nanowires, including conductivity, carrier mobility, and charge dynamics. Coating-induced heterojunctions can generate internal electric fields that promote directional charge separation and improve electronic response. A representative example is the graphene/4H-SiC nanowire array Schottky junction, in which the built-in field at the interface enables efficient carrier separation and self-powered ultraviolet photodetection [94]. Similarly, ZnO-coated SiC nanowires prepared by thermal evaporation formed core-shell heterostructures with improved field emission characteristics, including lower turn-on fields and enhanced emission stability due to modified surface band structure and improved electron extraction [98]. Amorphous carbon-coated SiC nanowires also showed enhanced field emission performance, with a low turn-on field of 0.5 V $\mu m^{-1}$ and a threshold field of 2.1 V $\mu m^{-1}$, attributed to increased interfacial conductivity and reduced work function [99]. In addition, local defect or site-dependent states in nanostructured SiC can further influence electronic behavior [100].

 doi:10.20944/preprints202605.0609.v1



## 5. Applications and Limitations of Coated SiC Nanowires

### *5.1. Enhancement Properties and Applications of Coated SiC Nanowires*

The performance of SiC nanowires is significantly influenced by surface modification. While pristine SiC nanowires exhibit functional capabilities in sensing, energy storage, catalysis, and structural applications, coated or hybrid systems generally provide enhanced performance due to improved interfacial interactions. These modifications influence charge transport, surface activity, and operational stability, thereby expanding the application scope of SiC nanowires. Figure 12 schematically summarizes the representative application areas of coated and hybrid SiC nanowires.

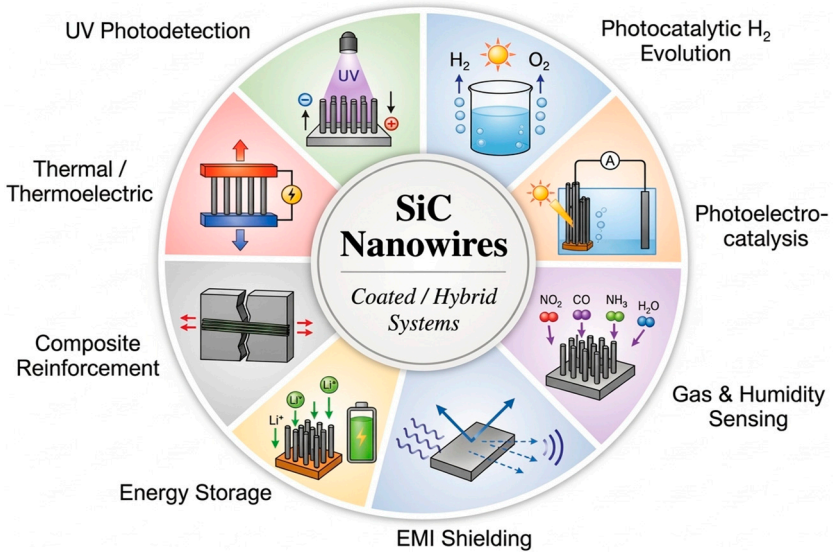


**Figure 12.** Schematic overview of the representative applications of coated and hybrid SiC nanowires.

#### 5.1.1. Ultraviolet Photodetection

Pristine SiC nanowires are intrinsically suitable for ultraviolet photodetection because of their wide bandgap (~3.2 eV) together with excellent thermal and chemical stability. Teker et al. reported single-nanowire UV detectors with rise and decay times on the order of 3–5 s [101]. Improved device design has further enhanced the performance of uncoated SiC nanowires; for example, Sun et al. developed a flexible and transparent SiC nanowire fabric that exhibited response times below 30 ms over the 260–510 nm range while maintaining mechanical flexibility under strains below 50% [102]. These results confirm that bare SiC nanowires already provide a robust platform for UV sensing.

Compared with pristine structures, coated SiC nanowires show clear advantages in photodetection performance because surface and interface modification can promote carrier separation and suppress recombination. Xue et al. reported a radial SiC/$SiO_2$/$SnO_2$ core-shell heterojunction device with a responsivity of 3.96 $A \cdot W^{-1}$ at 260 nm and a rapid response of about 9.3 ms, which was attributed to efficient charge separation across the multijunction interface [103]. Similarly, Li et al. demonstrated graphene-coated 4H-SiC nanowire arrays operating in a self-powered mode, with a response time below 5 ms and reduced dark current due to the built-in Schottky field at the graphene/SiC interface [94].

These findings indicate that, although uncoated SiC nanowires are already effective UV detectors, coating and interface engineering can further improve response speed, sensitivity, and dark-current suppression by enabling more efficient carrier transport and interfacial charge regulation.

#### 5.1.2. Photocatalytic Hydrogen Evolution

Pristine β-SiC nanowires can exhibit improved photocatalytic hydrogen evolution when their defect structure is optimized. Hao et al. reported defect-rich β-SiC nanowires with enhanced

 doi:10.20944/preprints202605.0609.v1



hydrogen-evolution activity under visible light, which was attributed to improved light absorption and more efficient charge separation, as supported by PL and UV–vis analyses [16].

However, interfacial modification provides a more effective enhancement strategy. Wang et al. demonstrated that Ni-loaded β-SiC nanowires achieved a hydrogen production rate of 375.4 $\mu mol \cdot g^{-1} \cdot h^{-1}$ at an optimal Ni loading of 0.05 wt.%, which was significantly higher than that of the uncoated sample. This improvement was attributed to the role of Ni in suppressing electron–hole recombination and facilitating electron transfer at the Ni–SiC interface [104].

These results indicate that, although defect engineering can improve the activity of pristine SiC nanowires, catalytic surface loading provides a more pronounced advantage by enhancing interfacial charge separation and reducing recombination losses.

#### 5.1.3. Photoelectrocatalysis

Pristine SiC nanowires have potential for photoelectrocatalytic applications because of their chemical stability and suitable electronic structure. However, their PEC performance has not been widely studied, and the available baseline data for uncoated SiC nanowires remain limited.

In contrast, coated SiC nanowires have shown improved PEC behavior. Liao et al. reported PEDOT:PSS-coated SiC nanowire films as photoanodes with higher photocurrent stability and better hole-transport efficiency [105]. In this system, the hybrid organic-inorganic interface promoted carrier separation and facilitated charge transfer at the electrode-electrolyte interface, thereby enhancing photoelectrocatalytic activity.

These findings suggest that, compared with the still limited PEC performance data of pristine SiC nanowires, coated SiC nanowires offer clearer advantages in interfacial charge transfer and operational stability. At the same time, the lack of direct comparison between pristine and coated SiC nanowires remains a research gap that should be addressed in future studies.

#### 5.1.4. Gas and Humidity Sensing

Pristine SiC nanowires are attractive for gas and humidity sensing because of their chemical stability and ability to operate at elevated temperatures. Teker et al. showed that uncoated SiC nanowires could detect $NO_2$ with response times of about 5 s at 250 °C [101]. Bur et al. further demonstrated SiC-FET gas sensors in which sensitivity and selectivity could be optimized by modulating temperature and gate bias [106]. In addition, Wang et al. developed capacitive humidity sensors based on nanoporous silicon pillars with SiC nanowires, which exhibited a linear humidity response attributed to dipolar surface interactions [107]. Peng et al. also reported conductance modulation in SiC nanowire field-effect transistors upon chemical adsorption, further confirming the sensing capability of pristine SiC nanowires [108]. Together, these studies show that uncoated SiC nanowires already provide a stable platform for gas and humidity sensing.

Compared with pristine SiC nanowires, coated SiC nanowires can offer improved sensing performance through enhanced surface reactivity and interfacial charge transfer. Chen et al. reported Pt-decorated SiC nanowires for hydrogen sensing at 500 °C, where Pt significantly improved sensor response and stability [96]. This enhancement was attributed to catalytic hydrogen dissociation on Pt and more efficient charge transfer across the Pt–SiC interface. These results indicate that, although bare SiC nanowires are already effective sensing materials, surface modification with catalytic coatings can further improve sensitivity, response stability, and high-temperature sensing performance.

#### 5.1.5. Electromagnetic Interference Shielding

In their uncoated form, SiC nanowires exhibit electromagnetic interference (EMI) shielding capability primarily through dielectric relaxation and interfacial polarization mechanisms. Shen et al. reported that uncoated SiC nanowires exhibit moderate EMI shielding behavior, indicating that they can already provide a useful dielectric contribution to electromagnetic attenuation [109].

 doi:10.20944/preprints202605.0609.v1



Compared with uncoated SiC nanowires, coated and hybrid structures exhibit much stronger EMI shielding performance. Guo et al. reported SiC@carbon nanowire aerogels with shielding effectiveness above 50 dB, which was attributed to the combined effects of multiple reflection, conductive loss, and interfacial polarization within the porous conductive network [110]. Similarly, Liang et al. incorporated SiC nanowires into graphene/PVDF composite films and achieved shielding effectiveness above 40 dB together with high thermal conductivity [111]. These results indicate that, although pristine SiC nanowires can contribute to EMI attenuation through dielectric effects, surface modification and hybridization provide clearer advantages by improving conductivity, strengthening interfacial polarization, and broadening the attenuation capability of the shielding material.

#### 5.1.6. Energy Storage

Without surface modification, β-SiC nanowires have already been considered as promising anode materials for lithium-ion batteries because their one-dimensional morphology provides short $Li^+$ diffusion pathways together with good structural stability. Vishnu et al. reported a reversible capacity of about 1000 $mAh \cdot g^{-1}$, highlighting the intrinsic mechanical robustness and electrochemical stability of uncoated SiC nanowires [112].

Compared with bare SiC nanowires, modified SiC nanowire systems show clearer electrochemical advantages. Gonzalez et al. showed that Li decoration improved the electronic structure and bonding characteristics of SiC nanowires, making them more favorable for energy-storage applications [113]. Likewise, Li et al. reported quasi-aligned SiC@C nanowire arrays as binder-free micro-supercapacitor electrodes with enhanced areal capacitance and mechanical stability [114]. Chen et al. further demonstrated that nitrogen-doped SiC nanoarrays exhibited high-rate capability and excellent cycling performance because of improved charge transport and defect-assisted electrochemical activity [115]. These results indicate that, although uncoated SiC nanowires already provide a stable structural framework for energy storage, surface modification and doping are more effective for enhancing conductivity, increasing active sites, and improving overall electrochemical performance.

#### 5.1.7. Composite Reinforcement

SiC nanowires are promising reinforcements for structural composites because of their high aspect ratio, mechanical strength, and crack-bridging capability. Wong et al. showed that single uncoated SiC nanowires possess high tensile strength and elasticity, confirming their ability to improve load transfer and energy dissipation in composite systems [116].

Compared with uncoated SiC nanowires, surface-modified or coated SiC nanowires provide additional mechanical advantages by improving interfacial compatibility with the surrounding matrix. Yang et al. reported that carbon-coated SiC nanowires enhanced the strength and toughness of SiC ceramics through stronger interfacial bonding and more effective stress distribution [77]. Similarly, Chu et al. incorporated SiC nanowires into SiC coatings for C/C composites and achieved improved mechanical integrity together with enhanced thermal shock and oxidation resistance [79]. These results indicate that, although uncoated SiC nanowires already provide effective mechanical reinforcement, coated SiC nanowires are more advantageous because they optimize interfacial bonding, reduce stress concentration, and improve the overall reliability of the composite system.

#### 5.1.8. Thermal and Thermoelectric Applications

SiC nanowires are relevant to thermal and thermoelectric applications because of their high thermal stability and size-dependent phonon transport behavior. Takahashi et al. directly measured the thermal conductivity of β-SiC nanowires using a four-point 3-ω probe method and reported values of 82 $W \cdot m^{-1} \cdot K^{-1}$ for single nanowires and 73 $W \cdot m^{-1} \cdot K^{-1}$ for double nanowire systems, both of which are significantly lower than those of bulk SiC [117]. Consistent with this trend, Papanikolaou theoretically predicted that the lattice thermal conductivity of SiC nanowires should be much lower

 doi:10.20944/preprints202605.0609.v1



than that of bulk SiC because of enhanced phonon scattering at the nanoscale [118]. These studies indicate that bare SiC nanowires already possess intrinsic thermal-transport characteristics of interest for thermoelectric design.

Compared with bare SiC nanowires, hybrid SiC-nanowire systems have shown clearer advantages in thermal-management applications, although direct evidence for coated SiC nanowires in thermoelectric conversion remains limited. For example, hybrid composites containing SiC nanowires have been reported to improve heat conduction by constructing more effective thermal transport pathways, as demonstrated in SiC-nanowire-modified C/C composites and graphene/SiC-nanowire/PVDF systems [119,120]. hese findings suggest that hybridization can provide additional control over interfacial heat transport and thermal conductivity, but the thermoelectric potential of coated or hybrid SiC nanowires is still underexplored and requires more direct study.

### *5.2. Current Limitations and Technical Challenges*

Although coated and hybrid SiC nanowires have promising applications, there are a number of challenges to their adoption. These are associated with problems in reliability in coating, scalability in synthesis, cost of fabricating and integrating the device.

#### 5.2.1. Coating Reliability and Stability

A major issue that has remained in coated SiC nanowires is maintaining interfacial stability in the extreme operating conditions. Sha et al. developed the gradient lamellar networks of SiC nanowires with heavy oxide coating to protect thermal systems in reusable form. Although they offered better thermal stability and oxidation resistance, the authors also highlighted that thermal mismatch between the ceramic shell and the nanowire core can still result in interfacial delamination and long-term degradation, particularly in the case of repeated thermal cycling [121].

#### 5.2.2. Scalability and Uniformity of Coating Processes

Traditional synthesis methods like chemical vapor deposition (CVD) and in situ growth methods can also produce quality coating but are constrained in terms of scalability because of slow deposition speeds and temperature limitations. Recently, Yu et al. have developed continuous networks of SiC nanowires through an in-situ growth technique that is scalable. They have however observed that the uniformity of coating thickness and morphology across large areas is a bottleneck to large scale production [122].

#### 5.2.3. Fabrication Cost and Processing Complexity

Multi-step procedures such as catalyst-enhanced nanowires growth, surface modification, and after-treatment are usually necessary to produce hybrid SiC nanostructures. Jin et al. also reported the development of SiC nanowire coating on carbon/carbon composites by an in situ catalytic reaction and this made the whole process easier. However, the technique still needed to be processed under high temperature and inert gases which may raise the cost and power consumption of fabrication [123].

#### 5.2.4. Integration Challenges in Composite and Electronic Systems

Incorporating coated SiC nanowires into functional composites or devices presents further difficulties related to interfacial adhesion and mechanical compatibility. Li et al. investigated HfC ceramic coatings toughened with SiC nanowires and found that although the addition of nanowires enhanced ablation resistance, interfacial stress during thermal cycling contributed to crack initiation and reduced structural durability [124]. These observations underscore the importance of interface engineering for reliable device-level integration.

 doi:10.20944/preprints202605.0609.v1



## 6. Conclusions and Outlook

Coated and hybrid SiC nanowires have shown significant promise across various high-performance applications due to their enhanced functional properties. The development of coated and hybrid SiC nanowires will rely on the strategic development of structural engineering, intelligent sensing integration and computationally informed material development. These guidelines will help overcome existing drawbacks and expand the range of applications of SiC-based nanomaterials. While notable progress has been made in synthesis and application development, challenges such as coating stability, scalability, and long-term performance remain. Future research should prioritize interface control, multifunctional integration, and data-driven design approaches. With continued advancement, these engineered nanostructures are well-positioned to play a critical role in next-generation technologies operating under extreme conditions.

A key area of research is the design of structurally integrated, hybrid nanowires e.g., core shell and multilayer structures, that combine high-temperature stability of SiC with improved electrical, catalytic or interfacial performance. According to Liu et al., carbon nanotube-coated SiC nanowires showed a better electrical conductivity and electromagnetic shielding capability, which proves the possibility of such structures in multifunctional nanodevices [125].

The future research in sensing technologies is to create smart and multifunctional sensor systems using coated SiC nanowires. Although high-temperature sensors have been proven to work, some additional research is required in order to allow them to be incorporated into wireless, self-powered, and autonomous systems in both aerospace and industry [126]. In addition, there have been recent advances in flexible SiC-based sensors, which implies the use of wearable and biomedical applications, but the problems of long-term stability and signal quality have not been resolved [127].

Artificial intelligence (AI) provides a good opportunity to design coated SiC nanowires as it predicts the compatibility of the coating, the quality of the interface, and the functionality. Even though not used extensively to this system yet, AI techniques have demonstrated success in other nanomaterials and would be useful in developing improved hybrid SiC structures [128].

**Author Contributions:** Conceptualization, M.I., B.L. and J.C.; methodology, M.I.; validation, B.L. and J.C.; formal analysis, M.I., X.S. and Y.L.; investigation, M.I.; data curation, M.I., X.S. and B.Z.; writing—original draft preparation, M.I.; writing—review and editing, B.L. and J.C.; visualization, M.I., X.S. and Y.L.; supervision, B.L. and J.C.; project administration, B.L. and J.C. All authors have read and agreed to the published version of the manuscript.

**Funding:** This research received the funding of National Nature Science Foundation of China (No. 52172014).

**Data Availability Statement:** No new data were created or analyzed in this study. Data sharing is not applicable to this article.

**Acknowledgments:** The authors express their appreciation to National Nature Science Foundation of China (No. 52172014).

**Conflicts of Interest:** The authors declare no conflicts of interest.

## References

1. Samykano M. Progress in one-dimensional nanostructures. *Mater. Charac.* **2021**, *179*, 111373.
2. Nanowires CS. A Laser Ablation Method for the Synthesis of Crystalline Semiconductor Nanowires. *Science* **1998**, *279*, 208–208.
3. Cui Y, Wei Q, Park H, Lieber CM. Nanowire Nanosensors for Highly Sensitive and Selective Detection of Biological and Chemical Species. *Science*. **2001**, *293*, 1289–1292.
4. Wang ZL. ZnO nanowire and nanobelt platform for nanotechnology. *Mat. Sci. Eng. R.* **2009**, *64*, 33–71.
5. Kimoto T, Cooper JA. *Fundamentals of silicon carbide technology: growth, characterization, devices and applications,* John Wiley & Sons: 1 Fusionopolis Walk #07-01 Solaris South Tower, Singapore, 2014; pp. 11–33.

 doi:10.20944/preprints202605.0609.v1




6. Saddow SE. *Silicon carbide biotechnology: a biocompatible semiconductor for advanced biomedical devices and applications*, 2nd ed Elsevier: Radarweg 29, PO Box 211, 1000 AE Amsterdam, Netherlands, The Boulevard, Langford Lane, Kidlington, Oxford OX5 1GB, UK, 50 Hampshire Street, 5th Floor, Cambridge, MA 02139, USA, 2016; pp. 1–25.
7. Yibibulla T, Jiang Y, Wang S, Huang H. Size-and temperature-dependent Young's modulus of SiC nanowires determined by a laser-Doppler vibration measurement. *Appl. Phys. Lett.* **2021,** *118,* 043103.
8. Pei B, Zhu Y, Yuan M, Huang Z, Li Y. Effect of in situ grown SiC nanowires on microstructure and mechanical properties of C/SiC composites. *Ceram. Int*. **2014,** *40,* 5191–5195.
9. Casady JB, Johnson RW. Status of silicon carbide (SiC) as a wide-bandgap semiconductor for high-temperature applications: A review. *Solid State Electron.* **1996**, *39,* 1409–1422.
10. Zekentes K, Choi J, Stambouli V, Bano E, Karker O, Rogdakis K. Progress in SiC nanowire field-effect-transistors for integrated circuits and sensing applications. *Microelectron. Eng.* **2022,** *255,* 111704.
11. Wang Y, Zhang J, Wu T, Huang G. Advance understanding of the synthesis process, special performance, and multidiscipline applications of SiC nanowires and the constructed composites. *J. Mater. Res. Technol.* **2024,** *29,* 1131–1154.
12. Wu R, Li B, Gao M, Chen J, Zhu Q, Pan Y. Tuning the morphologies of SiC nanowires via the control of growth temperature, and theirphotoluminescence properties. *Nanotechnology* **2008,** *19,* 335602.
13. Singh R. Reliability and performance limitations in SiC power devices. *Microelectron. Reliab.* **2006,** *46,* 713–730.
14. Zekentes K, Rogdakis K, Bano E, editors. Material limitations for the development of high performance SiC NWFETs. *Materials Science Forum* **2012,** *711,* 70–74.
15. Qiang X, Li H, Zhang Y, Wang Z, Ba Z, Zhang X. Mechanical and oxidation protective properties of SiC nanowires-toughened SiC coating prepared in-situ by a CVD process on C/C composites. *Surf. Coat. Tech.* **2016,** *307,* 91–98.
16. Hao J, Wang Y, Tong X, Jin G, Guo X. Photocatalytic hydrogen production over modified SiC nanowires under visible light irradiation. *Int. J. Hydrogen Energ.* **2012,** *37,* 15038–15044.
17. Wang L, Wu J, Shang M, Gao F, Li X, Zheng Y, Yang W, Chen S. Improved piezoresistive properties of ZnO/SiC nanowire heterojunctions with an optimized piezoelectric nanolayer. *J. Mater. Sci.* **2021,** *56,* 17146–17155.
18. Fotovvati B, Namdari N, Dehghanghadikolaei A. On coating techniques for surface protection: A review. *J. Manuf. Mater. Proc.* **2019,** *3,* 28.
19. Liu B, Yin Q, Chen X, He B, Liu L, Yang L, Zhao X, Yang B, Xu B, Jiang W. Theoretical and experimental study of the mechanism for preparation of SiC nanowires by carbothermal reduction. *J. Phys. Chem. Solids* **2024,** *187,* 111886.
20. Shen Z, Chen J, Li B, Li G, Li J, Hou X. A novel two-stage synthesis for 3C–SiC nanowires by carbothermic reduction and their photoluminescence properties. *J. Mater. Sci.* **2019,** *54,* 12450–12462.
21. Yang G, Wu R, Chen J, Pan Y, Zhai R, Wu L, Jing L. Growth of SiC nanowires/nanorods using a Fe–Si solution method. *Nanotechnology* **2007,** *18,* 155601.
22. Lee J, Byeun Y, Lee S, Choi S. In situ growth of SiC nanowires by carbothermal reduction using a mixture of low-purity $SiO_2$ and carbon. *J. Alloy. Compound.* **2008,** *456,* 257–263.
23. Yao X, Tan S, Huang Z, Dong S, Jiang D. Growth mechanism of β-SiC nanowires in SiC reticulated porous ceramics. *Ceram. Int.* **2007,** *33,* 901–904.
24. Liu S, Liu H, Huang Z, Fang M, Liu Y, Wu X. Synthesis of β-SiC nanowires via a facile CVD method and their photoluminescence properties. *RSC Adv.* **2016,** *6,* 24267–24272.
25. Fu Q, Li H, Shi X, Li K, Wei J, Hu Z. Synthesis of silicon carbide nanowires by CVD without using a metallic catalyst. *Mater. Chem. Phys.* **2006,** *100,* 108–111.
26. Gu X, Qiang Y, Zhao Y. Synthesis, structural and electrical properties of SiC nanowires via a simple CVD method. *J. Mater. Sci- Mater. El.* **2012,** *23,* 1037–1040.
27. Li Z, Zhang J, Meng A, Guo J. Large-area highly-oriented SiC nanowire arrays: synthesis, Raman, and photoluminescence properties. *J. Phys. Chem. B* **2006,** *110,* 22382–22386.

 doi:10.20944/preprints202605.0609.v1




28. Xi G, He Y, Wang C. Molecular Template Assisted Growth of Ultrathin Silicon Carbide Nanowires with Strong Green Light Emission and Excellent Field-Emission Properties. *Chem. Eur. J.* **2010,** *16,* 5184–5190.
29. Jun D, Zhu H, Li G, Deng C, Li J. Growth of SiC nanowires on wooden template surface using molten salt media. *Appl. Surf. Sci.* **2014,** *320,* 620–626.
30. Zou X, Ji L, Lu X, Zhou Z. Facile electrosynthesis of silicon carbide nanowires from silica/carbon precursors in molten salt. *Sci. Rep-UK.* **2017,** *7,* 9978.
31. Shi W, Zheng Y, Peng H, Wang N, Lee CS, Lee ST. Laser ablation synthesis and optical characterization of silicon carbide nanowires. *J. Am. Ceram. Soc.* **2000,** *83,* 3228–3230.
32. Kokai F, Uchiyama K, Shimazu T, Koshio A. Fabrication of two types of one-dimensional Si–C nanostructures by laser ablation. *Appl. Phys. A-Mater.* **2010,** *101,* 497–502.
33. Li K, Wei J, Li H, Li Z, Hou D, Zhang Y. Photoluminescence of hexagonal-shaped SiC nanowires prepared by sol–gel process. *Mat. Sci. Eng. A* **2007,** *460,* 233–237.
34. Mishra SB, Mishra AK, Krause RW, Mamba BB. Synthesis of Silicon Carbide Nanowires from a Hybrid of Amorphous Biopolymer and Sol–Gel-Derived Silica. *J. Am. Ceram. Soc.* **2009,** *92,* 3052–3058.
35. Wei J, Zhang Y, Li X, Zhang H, Guo Y, Wang T, Qian X, Lei W. Recent progress in synthesis, growth mechanisms, and electromagnetic wave absorption properties of silicon carbide nanowires. *Ceram. Int.* **2022,** *48,* 35966–35985.
36. Cheong K, Lockman Z. Effects of temperature and crucible height on the synthesis of 6H-SiC nanowires and nanoneedles. *J. Alloy. Compound.* **2009,** *481,* 345–348.
37. Guo C, Cheng L, Ye F, Zhang Q. Adjusting the Morphology and Properties of SiC Nanowires by Catalyst Control. *Materials* **2020,** *13,* 5179.
38. Lin H, Li H, Wang T, Shen Q, Shi X, Feng T. Influence of temperature and oxygen on the growth of large-scale SiC nanowires. *CrystEngComm* **2019,** *21,* 1801–1808.
39. Huang C, Lee J, Wang C. On the 2H-to 3C-type transformation and growth mechanism of SiC nanowires upon carbothermal reduction of rice straws. *ACS Omega* **2022,** *7,* 5039–5052.
40. Krishnan B, Thirumalai RVK, Koshka Y, Sundaresan S, Levin I, Davydov AV, Merrett JV. Substrate-dependent orientation and polytype control in SiC nanowires grown on 4H-SiC substrates. *Cryst. Growth Des.* **2011,** *11,* 538–541.
41. He J, Sun B, Sun Y, Wang C. Selective growth of zinc blende, wurtzite and hybrid SiC nanowires via a simple chemical vapor deposition route. *CrystEngComm.* **2019,** *21,* 4740–4746.
42. Wang H, Lin L, Yang W, Xie Z, An L. Preferred Orientation of SiC Nanowires Induced by Substrates. *J. Phys. Chem. C* **2010,** *114,* 2591–2594.
43. Chen B, Chi C, Hsu W, Ouyang H. Synthesis of SiC/$SiO_2$ core–shell nanowires with good optical properties on Ni/$SiO_2$/Si substrate via ferrocene pyrolysis at low temperature. *Sci. Rep-UK.* **2021,** *11,* 233.
44. Li L, Chu Y, Li H, Qi L, Fu Q. Periodically twinned 6H-SiC nanowires with fluctuating stems. *Ceram. Int.* **2014,** *40,* 4455–4460.
45. Zhang H, Wang C, Wang L. Helical Crystalline SiC/$SiO_2$ Core−Shell Nanowires. *Nano Lett.* **2002,** *2,* 941–944.
46. Morresi T, Timpel M, Pedrielli A, Garberoglio G, Tatti R, Verucchi R, et al. A novel combined experimental and multiscale theoretical approach to unravel the structure of SiC/$SiO_x$ core/shell nanowires for their optimal design. *Nanoscale* **2018,** *10,* 13449–13461.
47. Cheng G, Chang T, Qin Q, Huang H, Zhu Y. Mechanical properties of silicon carbide nanowires: effect of size-dependent defect density. *Nano Lett.* **2014,** *14,* 754–758.
48. Wang Z, Zu X, Gao F, Weber WJ. Atomistic simulations of the mechanical properties of silicon carbide nanowires. *Phys. Rev. B* **2008,** *77,* 224113.
49. Ma J, Liu Y, Hao P, Wang J, Zhang Y. Effect of different oxide thickness on the bending Young's modulus of $SiO_2$@SiC nanowires. *Sci. Rep-UK* **2016,** 6, 18994.
50. Perisanu S, Gouttenoire V, Vincent P, Ayari A, Choueib M, Bechelany M, Cornu D, Purcell1 S. Mechanical properties of SiC nanowires determined by scanning electron and field emission microscopies. *Phys. Rev. B* **2008,** *77,* 165434.
51. Li J, Shirai T, Fuji M. Silicon Carbide and Its Nanostructures. *Annual Report of the Advanced Ceramics Research Center Nagoya Institute of Technology,* **2014,** *3,* 5–10.

 doi:10.20944/preprints202605.0609.v1




52. Ramakers S, Marusczyk A, Amsler M, Eckl T, Mrovec M, Hammerschmidt T, Drautz R. Effects of thermal, elastic, and surface properties on the stability of SiC polytypes. *Phys. Rev. B* **2022,** *106,* 075201.
53. Rurali R. Electronic and structural properties of silicon carbide nanowires. *Phys. Rev. B* **2005,** *71,* 205405.
54. Zhou W, Liu X, Zhang Y. Simple approach to β-SiC nanowires: synthesis, optical, and electrical properties. *Appl. Phys. Lett.* **2006,** *89,* 223124.
55. Chen J, Tang W, Xin L, Shi Q. Band gap characterization and photoluminescence properties of SiC nanowires. *Appl. Phys. A* **2011,** *102,* 213–217.
56. Hu P, Dong S, Zhang X, Gui K, Chen G, Hu Z. Synthesis and characterization of ultralong SiC nanowires with unique optical properties, excellent thermal stability and flexible nanomechanical properties. *Sci. Rep-UK* **2017,** *7,* 3011.
57. Sultan NM, Albarody TMB, Al-Jothery HKM, Abdullah MA, Mohammed HG, Obodo KO. Thermal Expansion of 3C-SiC Obtained from In-Situ X-ray Diffraction at High Temperature and First-Principal Calculations. *Materials* **2022,** *15,* 6229.
58. Hossain ZM, Elahi F, Zhang Z. Differential anharmonicity and thermal expansion coefficient in 3C-SiC nanowires. *Phys. Rev. B* **2019,** *99,* 115407.
59. Lee KM, Choi TY, Lee SK, Poulikakos D. Focused ion beam-assisted manipulation of single and double β-SiC nanowires and their thermal conductivity measurements by the four-point-probe 3-ω method. *Nanotechnology* **2010,** *21,* 125301.
60. Valentín L, Betancourt J, Fonseca L, Pettes M, Shi L, Soszyński M, Huczko A. A comprehensive study of thermoelectric and transport properties of β-silicon carbide nanowires. *J. Appl. Phys.* **2013,** *114,* 184301.
61. Termentzidis K, Barreteau T, Ni Y, Merabia S, Zianni X, Chalopin Y, Chantrenne P, Volz S. Modulated SiC nanowires: Molecular dynamics study of their thermal properties. *Phys. Rev. B* **2013,** *87,* 125410.
62. Yin K, Shi L, Ma X, Zhong Y, Li M, He X. Thermal Conductivity of 3C/4H-SiC Nanowires by Molecular Dynamics Simulation. *Nanomaterials* **2023,** *13,* 2196.
63. Liu Y, Li G, Huan L, Cao S. Advancements in silicon carbide-based supercapacitors: materials, performance, and emerging applications. *Nanoscale* **2024,** *16,* 504–526.
64. Maboudian R, Carraro C, Senesky DG, Roper CS. Advances in silicon carbide science and technology at the micro- and nanoscales. *J. Vac. Sci. Technol. A* **2013,** *31,* 050805.
65. Wu R, Zhou K, Yue CY, Wei J, Pan Y. Recent progress in synthesis, properties and potential applications of SiC nanomaterials. *Prog. Mater. Sci.* **2015,** *72,* 1–60.
66. Chase MW. NIST-JANAF thermochemical tables. *Journal of physical and chemical reference data* **1998,** *28,* 1951.
67. Zhao J, Li Z, Zhang M, Meng A. Super-hydrophobic surfaces of $SiO_2$-coated SiC nanowires: Fabrication, mechanism and ultraviolet-durable super-hydrophobicity. *J. Colloid Interf. Sci.* **2015,** *444,* 33–37.
68. Niu F, Wang Y, Wang Y, Ma L, Liu J, Wang C. A crack-free SiC nanowire-toughened Si-Mo-WC coating prepared on graphite materials for enhancing the oxidation resistance. *Surf. Coat. Tech.* **2018,** *344,* 52–57.
69. Zhang Y, Yang B, Zhang P, Zhang J, Ren J, Hu Z. SiC nanowire toughened $ZrB_2$–SiC ablative coating for SiC coated C/C composites. *Ceram. Int.* **2015,** *41,* 14579–14584.
70. Lu D, Zhuang L, Yang Y, Jia S, Su L, Zhang P, Qin Y, Niu M, Peng K, Wang H. Strong and Tough Porous Silicon Carbide Ceramics. *ACS Nano* **2025,** *19,* 18313–18321.
71. Amato M, Rurali R. Surface physics of semiconducting nanowires. *Prog. Surf. Sci.* **2016,** *91,* 1–28.
72. Liang C, Wang Z. Controllable fabricating dielectric–dielectric SiC@C core–shell nanowires for high-performance electromagnetic wave attenuation. *ACS Appl. Mater. Interfaces* **2017,** *9,* 40690–40696.
73. Liao X, Chen J, Wang M, Liu Z, Ding L, Li Y. Enhanced photocatalytic and photoelectrochemical activities of $SnO_2$/SiC nanowire heterostructure photocatalysts. *J. Alloy. Compound.* **2016,** 658, 642–648.
74. Wang M, Chen J, Liao X, Liu Z, Zhang J, Gao L, Ye L. Highly efficient photocatalytic hydrogen production of platinum nanoparticle-decorated SiC nanowires under simulated sunlight irradiation. *Int. J. Hydrogen Energ.* **2014,** *39,* 14581–14587.
75. Peng Y, Han G, Wang D, Wang K, Guo Z, Yang J, Yuan W. Improved $H_2$ evolution under visible light in heterostructured SiC/CdS photocatalyst: Effect of lattice match. *Int. J. Hydrogen Energ.* **2017,** *42,* 14409–14417.
76. Wang B, Zhang J, Huang F. Enhanced visible light photocatalytic $H_2$ evolution of metal-free g-$C_3N_4$/SiC heterostructured photocatalysts. *Appl. Surf. Sci.* **2017,** *391,* 449–456.

 doi:10.20944/preprints202605.0609.v1




77. Yang W, Araki H, Tang C, Thaveethavorn S, Kohyama A, Suzuki H, Noda T. Single-crystal SiC nanowires with a thin carbon coating for stronger and tougher ceramic composites. *Adv. Mater.* **2005,** *17,* 1519–1523.
78. Tang C, Bando Y, Sato T, Kurashima K, Ding X, Gan Z, Qi S. SiC and its bicrystalline nanowires with uniform BN coatings. *Appl. Phys. Lett.* **2002,** *80,* 4641–4643.
79. Chu Y, Fu Q, Li H, Wu H, Li K, Tao J, Lei Q. SiC coating toughened by SiC nanowires to protect C/C composites against oxidation. *Ceram. Int.* **2012,** *38,* 189–194.
80. Xie A, Zhang B, Ge Y, Peng K, Xu P, Wang X, Feng Z, Yi M, Zhou Z. Effect of the incorporation of SiC nanowire with double protective layers on SiC coating for C/C composites. *J. Eur. Ceram. Soc.* **2023,** *43,* 4636–4644.
81. Tak Y, Yong K. $ZrO_2$-coated SiC nanowires prepared by plasma-enhanced atomic layer chemical vapor deposition. *Surf. Rev. Lett.* **2005,** *12,* 215–219.
82. Ma J, Liu Y, Hao P, Wang J, Zhang Y. Effect of different oxide thickness on the bending Young's modulus of $SiO_2$@ SiC nanowires. *Sci. Rep-UK* **2016,** *6,* 18994.
83. Hu P, Dong S, Zhang D, Fang C, Zhang X. Catalyst-assisted synthesis of core–shell SiC/$SiO_2$ nanowires via a simple method. *Ceram. Int.* **2016,** *42,* 1581–1587.
84. Liu B, Sun J, Zhou L, Zhang P, Yan C, Fu Q. Microstructure evolution and growth mechanism of core-shell silicon-based nanowires by thermal evaporation of SiO. *J. Adv. Ceram.* **2022,** *11,* 1417–1430.
85. Zhuang L, Fu Q, Ma W, Zhang Y, Yan N, Song Q, Zhang Q. Oxidation protection of C/C composites: Coating development with thermally stabile SiC@PyC nanowires and an interlocking $TaB_2$-SiC structure. *Corros. Sci.* **2019,** *148,* 307–316.
86. Morresi T, Timpel M, Pedrielli A, Garberoglio G, Tatti R, Verucchi R, Pasquali L, Pugno N, Nardi M, Taioliet S. A novel combined experimental and multiscale theoretical approach to unravel the structure of SiC/$SiO_x$ core/shell nanowires for their optimal design. *Nanoscale* **2018,** *10,* 13449–13461.
87. Ferrand D, Cibert J. Strain in crystalline core-shell nanowires. *Eur. Phys. J-Appl. Phys.* **2014,** *67,* 30403.
88. Krasnitckii SA, Smirnov AM, Gutkin MY. Misfit stress and energy in composite nanowire with polygonal core. *Int. J. Eng. Sci.* **2023,** *193,* 103959.
89. Yang X, Ying L, Hua-fei C, Feng C. The degradation behavior of SiC coated PIP-C/SiC composites in thermal cycling environment. *Compos. Part B-Eng.* **2015,** *79,* 204–208.
90. Qiao Y, He G, Huang Z, HuangFu H, Li Z, Ju L, Shi Z, Yuan H. $TiO_2$ nanotube-coated hierarchical SiC nanowires as novel electrode materials with enhanced electrochemical performances for supercapacitors. *J. Mater. Chem. A* **2025,** *13,* 10197–10213.
91. Minami K, Kobinata K, Yan J. Multilayer Graphene-Coated Silicon Carbide Nanowire Formation Under Defocused Laser Irradiation. *Nanomanufacturing and Metrology* **2023,** *6,* 21.
92. Rufangura P, Khodasevych I, Agrawal A, Bosi M, Folland TG, Caldwell JD, Iacopi F. Enhanced absorption with graphene-coated silicon carbide nanowires for mid-infrared nanophotonics. *Nanomaterials* **2021,** *11,* 2339.
93. LI P, Liu Z, Xia Z, Yang J. Phosphotungstic acid/silicon carbide nanowire heterostructure photocatalyst for improving photodegradation of Rhodamine B. *Optoelectron. Adv. Mat.* **2023,** *17,* 170–176.
94. Li L, Wei G, Zhu P, Su Y, Ding L, Ma S, Xu B, Wang Y, Yang Y. Self-powered graphene/4H-SiC nanowire array-based ultraviolet photodetectors with fast response time and low dark current for promising wireless ultraviolet communication. *Appl. Mater. Today* **2024,** *37,* 102114.
95. Li P, Guo J, Ji X, Xiong Y, Lai Q, Yao S, Zhu Y, Zhang Y, Xiao P. Construction of direct Z-scheme photocatalyst by the interfacial interaction of $WO_3$ and SiC to enhance the redox activity of electrons and holes. *Chemosphere* **2021,** *282,* 130866.
96. Chen J, Zhang J, Wang M, Li Y. High-temperature hydrogen sensor based on platinum nanoparticle-decorated SiC nanowire device. *Sensor. Actuat. B-Chem.* **2014,** *201,* 402–406.
97. Jiang M, Liu Z, Ding L, Chen J. Facile fabrication and efficient photoelectrochemical water-splitting activity of electrodeposited nickel/SiC nanowires composite electrode. *Catal. Commun.* **2017,** *96,* 46–49.
98. Tak Y, Ryu Y, Yong K. Atomically abrupt heteronanojunction of ZnO nanorods on SiC nanowires prepared by atwo-step process. *Nanotechnology* **2005,** *16,* 1712.

 doi:10.20944/preprints202605.0609.v1




99. Zhang M, Li Z, Zhao J, Gong L, Meng A, Liu X, Fan X, Qi X. Amorphous carbon coating for improving the field emission performance of SiC nanowire cores. *J. Mater. Chem. C* **2015,** *3,* 658–663.
100. Joshi T, Dev P. Site-Dependent Properties of Quantum Emitters in Nanostructured Silicon Carbide. *PRX Quantum* **2022,** *3,* 020325.
101. Teker K. Photoresponse characteristics of silicon carbide nanowires. *Microelectron. Eng.* **2016,** *162,* 79–81.
102. Sun B, Sun Y, Wang C. Flexible transparent and free-standing SiC nanowires fabric: stretchable UV absorber and fast-response UV-A detector. *Small* **2018,** *14,* 1703391.
103. Xue B, Wang P, Liu H, Tang Z, Yan Z, Su Y, Xu B, Ding L, Wei G, Wang Y, Yang Y. SiC/$SiO_2$/$SnO_2$ Single Core–shell Nanowire Ultraviolet Photodetector with Radial Heterojunction: A Promising Strategy to Break the Responsivity-Speed Trade-Off. *Small* **2025,** *21,* 2412618.
104. Wang Y, Yang S, Li X, Huang W, He Z, Fu X, Zhu L, Xu M. Highly active nickel-loaded β-SiC nanowire catalysts for photocatalytic $H_2$ production by water splitting. *AIP Adv.* **2023,** *13,* 125202.
105. Liao X, Liu Z, Ding L, Chen J, Tang W. Photoelectrocatalytic activity of flexible PEDOT–PSS/silicon carbide nanowire films. *RSC Adv.* **2015,** *5,* 99143–99147.
106. Bur C, Bastuck M, Spetz AL, Andersson M, Schuetze A. Selectivity enhancement of SiC-FET gas sensors by combining temperature and gate bias cycled operation using multivariate statistics. *Sensor. Actuat. B-Chem.* **2014,** *193,* 931–940.
107. Wang H, Wang Y, Hu Q, Li X. Capacitive humidity sensing properties of SiC nanowires grown on silicon nanoporous pillar array. *Sensor. Actuat. B-Chem.* **2012,** *166,* 451–456.
108. Peng G, Ma W, Huang X, Zhou Y, He Y, Yu X, He B. Electrical transport properties of single SiC NW-FET. *Advanced Materials Research.* **2013,** *704,* 281–286.
109. Shen Z, Chen J, Li B, Li G, Zhang Z, Hou X. Recent progress in SiC nanowires as electromagnetic microwaves absorbing materials. *J. Alloy. Compound.* **2020,** *815,* 152388.
110. Guo P, Su L, Jia S, Ni Z, Dai Z, Guo J, Wang X, Peng K, Wang H. Strong SiC@Carbon nanowire aerogel metamaterials for efficient electromagnetic interference shielding. *Carbon* **2024,** *229,* 119492.
111. Liang C, Hamidinejad M, Ma L, Wang Z, Park CB. Lightweight and flexible graphene/SiC-nanowires/poly (vinylidene fluoride) composites for electromagnetic interference shielding and thermal management. *Carbon* **2020,** *156,* 58–66.
112. Vishnu DSM, Sure J, Kim H, Kumar RV, Schwandt C. Solid state electrochemically synthesised β-SiC nanowires as the anode material in lithium ion batteries. *Energy Storage Mater.* **2020,** *26,* 234–241.
113. Gonzalez M, Salazar F, Trejo A, Miranda Á, Nava R, Pérez LA, Cruz-Irisson M. Exploring the electronic and mechanical properties of lithium-decorated silicon carbide nanowires for energy storage. *J. Energy Storage* **2023,** *62,* 106840.
114. Li X, Liu Q, Chen S, Li W, Liang Z, Fang Z, Yang W, Tian Y, Yang Y. Quasi-aligned SiC@C nanowire arrays as free-standing electrodes for high-performance micro-supercapacitors. *Energy Storage Mater.* **2020,** *27,* 261–269.
115. Chen Y, Zhang X, Xie Z. Flexible nitrogen doped SiC nanoarray for ultrafast capacitive energy storage. *ACS Nano* **2015,** *9,* 8054–8063.
116. Wong EW, Sheehan PE, Lieber CM. Nanobeam mechanics: elasticity, strength, and toughness of nanorods and nanotubes. *Science* **1997,** *277,* 1971–1975.
117. Lee K, Choi T, Lee S, Poulikakos D. Focused ion beam-assisted manipulation of single and double β-SiC nanowires and their thermal conductivity measurements by the four-point-probe 3-ω method. *Nanotechnology* **2010,** *21,* 125301.
118. Papanikolaou N. Lattice thermal conductivity of SiC nanowires. *J. Phys-Condens. Mat.* **2008,** *20,* 135201.
119. Zhu H, Liu B, Hou J, Wang R, Cong Y, Dong Z, Li B, Guo J, Li X. Significantly improved thermal conductivity of C/C composite by constructing 3D SiC nanowires network in carbon felt via vacuum thermal evaporation. *Carbon* **2024,** *229,* 119539.
120. Sun Y, Zhang F, Guo L, Zhu Z, Gao X, Feng W, Zheng Q. Thermally conductive nanocomposite with silicon carbide nanowire-bridged boron nitride skeleton for multifunctional thermal interface materials. *Compos Pa. Rt. A-Appl. S.* **2025,** *192,* 108775.

 doi:10.20944/preprints202605.0609.v1




121. Jia J, Lu D, Jia S, Ni Z, Su L, Niu M, Peng K, Wang H. Gradient Lamellar SiC Nanowire Networks with Dense Coating for High-Performance Reusable Thermal Protection Materials. *ACS appl. Mater. interfaces* **2025,** *17,* 27136–27143.
122. Yu C, Yuan K, Wang B, Niu M, Xuan W, Yue M, Kuang J, Wang Q. In-situ constructing continuous networks composed of SiC nanowires for enhancing the thermal conductivity of epoxy composites. *Ceram. Int.* **2024,** *50,* 41137–41144.
123. Jin M, Li Z, Li Y, Wu J, Gao Z, Zhao Y, Li P. Formation of silicon carbide nanowire coatings on C/C composites using an in situ catalytic strategy for improved oxidation resistance. *Ceram. Int.* **2024,** *50,* 909–919.
124. Li H, Wang Y, Fu Q, Chu Y. SiC Nanowires Toughed HfC Ablative Coating for C/C Composites. *J. Mater. Sci. Technol.* **2015,** *31,* 70–76.
125. Liu H, Zhang X, Li K, Cui Qa, Han L, Shen Q, Li H, Yin X. Construction of core-shell structured SiC nanowires@carbon nanotubes hybrid conductive network for supercapacitors and electromagnetic interference shielding. *Carbon* **2024,** *228,* 119411.
126. Hunter GW, A Brief Overview of Silicon Carbide Based Smart Sensor System Technologies for Planetary and Aeronautics Applications. Silicon Carbide (SiC) Materials & Devices Workshop, Fayetteville, AR, US, August 13, 2024.
127. Wadhwa A, Perrotton A, Taherian MH, Zirakjou A, Benavides-Guerrero J, Gratuze M, Vaussenat F, Bolduc M, Cloutier S. Flexible screen-printed sic-based humidity sensors. *Commun. Eng.* **2025,** *4,* 96.
128. Chávez-Angel E, Eriksen MB, Castro-Alvarez A, Garcia JH, Botifoll M, Avalos-Ovando O, Arbiol J, Mugarza A. Applied Artificial Intelligence in Materials Science and Material Design. *Adv. Intell. Syst.* **2025,** *7,* 2400986.